

A QUANTITATIVE DEPOSITIONAL MODEL OF A LARGE DISTRIBUTIVE FLUVIAL SYSTEM (MEGAFAN) WITH TERMINAL AEOLIAN INTERACTION: THE UPPER JURASSIC GUARÁ DFS IN SOUTHWESTERN GONDWANA

ADRIANO DOMINGOS DOS REIS,¹ CLAITON MARLON DOS SANTOS SCHERER,¹ AMANDA OWEN,²
FRANCYNE BOCHI DO AMARANTE,¹ JOÃO PEDRO FORMOLO FERRONATTO,¹ GEORGE PANTOPOULOS,³
EZEQUIEL GALVÃO DE SOUZA,⁴ MANOELA BETTAREL BÁLICO,⁵ AND CÉSAR ALEJANDRO GOSO AGUILAR⁶

¹Institute of Geosciences, Federal University of Rio Grande do Sul (UFRGS), Avenida Bento Gonçalves 9500, 43 137 Building, CEP 91501-970, Porto Alegre, RS, Brazil

²School of Geographical and Earth Sciences, University of Glasgow, Glasgow G12 8QQ, U.K.

³Department of Earth Sciences “Ardito Desio,” University of Milan, Via Mangiagalli 34, 20133 Milano, Italy

⁴Campus Caçapava do Sul, Federal University of Pampa (UNIPAMPA), Avenida Pedro Anunciação 111, Brazil

⁵Departament of Geology, Federal University of Santa Catarina (UFSC), Campus Universitário Reitor João David Ferreira Lima, Trindade, CEP 88040-900, Florianópolis, SC, Brazil

⁶Facultad de Ciencias, Universidad de la República, Iguá 4225 y Mataojo 11400, Montevideo, Uruguay

e-mail: adreis@hotmail.com

ABSTRACT: Recent studies have shown that distributive fluvial systems are the dominant fluvial forms in modern continental sedimentary basins, thus composing a large part of the stratigraphic record. This study provides a basin-scale architectural analysis of the Guará Formation, from the Upper Jurassic record of southwestern Gondwana, and attempts to compare the formation’s depositional model to those developed for distributive fluvial system (DFS) successions. This time interval is significant because it was a period of intense tectonic activity related to the Paraná–Etendeka plume and the Gondwana breakup. Quantitative analyses were performed on stratigraphic sections at 17 locations (exposing a total of 720 m of stratigraphy) located in southern Brazil and northern Uruguay, from a larger dataset of 64 locations (comprising a total of 1070 m of stratigraphy). Four facies associations were identified: perennial fluvial channel fills, ephemeral fluvial channel fills, floodplain deposits, and aeolian deposits, indicating a dryland climate. Spatial trends were analyzed along a downstream-oriented transect (NNE–SSW) across the system. Grain size, channel-body thickness, number of stories, and bar thickness decrease downstream, indicating a reduction in channel depth, flow capacity, and channelization of the fluvial system, interpreted to be associated with downstream-increasing bifurcation, infiltration, and evapotranspiration. Based on spatial trends and distribution of facies associations, the deposits are interpreted to have been accumulated from a large DFS which can be divided into four zones, from proximal to distal: Zone 1, dominated by perennial fluvial channels; Zone 2, a mixture of perennial and ephemeral channels; Zones 3 and 4, deposits situated externally of the fluvial channel belts dominated by aeolian and floodplain deposits prevailing in each zone, respectively. The Guará Formation likely records the stratigraphic signature of the largest distributive fluvial systems reconstructed from both modern and ancient datasets, and one of the first where fluvio–aeolian interaction is quantified. The Guará Formation DFS model presented herein is key to understanding paleoenvironmental, paleoclimatic, and geotectonic changes related to Gondwanan fragmentation.

INTRODUCTION

An analysis of modern continental sedimentary basins by Hartley et al. (2010) and Weissmann et al. (2010, 2015) indicates that distributive fluvial systems (DFSs) cover a major fraction of the Paraná basin area. These works suggest that DFSs should therefore constitute much of the fluvial rock record in continental basins. However, large system- to basin-scale studies are needed to determine the presence of DFSs using criteria such as the spatial variation of facies associations, grain size, and channel features (Davidson et al. 2013; Owen et al. 2015, 2019; Weissmann et al. 2015). Basin-scale studies of ancient fluvial successions are essential for developing and refining generic facies models and local drainage-basin

reconstruction (Ventra and Clarke 2018). Several works describe DFSs from the rock record (including (Kelly and Olsen 1993; Nichols and Hirst 1998; DeCelles and Cavazza 1999; Cain and Mountney 2009; Çiftçi and Bozkurt 2009; Galloway et al. 2011; Owen et al. 2015, 2019; Primm et al. 2018; Ciccioli et al. 2018; Aliyuda et al. 2019; Burnham and Hodgetts 2019; Dal’ Bó et al. 2019; Burnham et al. 2020)). However, few basin-scale quantitative analyses of deposits exist. Quantifying depositional elements to determine their downstream distribution is essential to understand the morphological and morphodynamic diversity of individual distributive fluvial systems, as well as how the stratigraphic expression of different systems varies within a basin in the geological record (e.g., Owen et al. 2019).

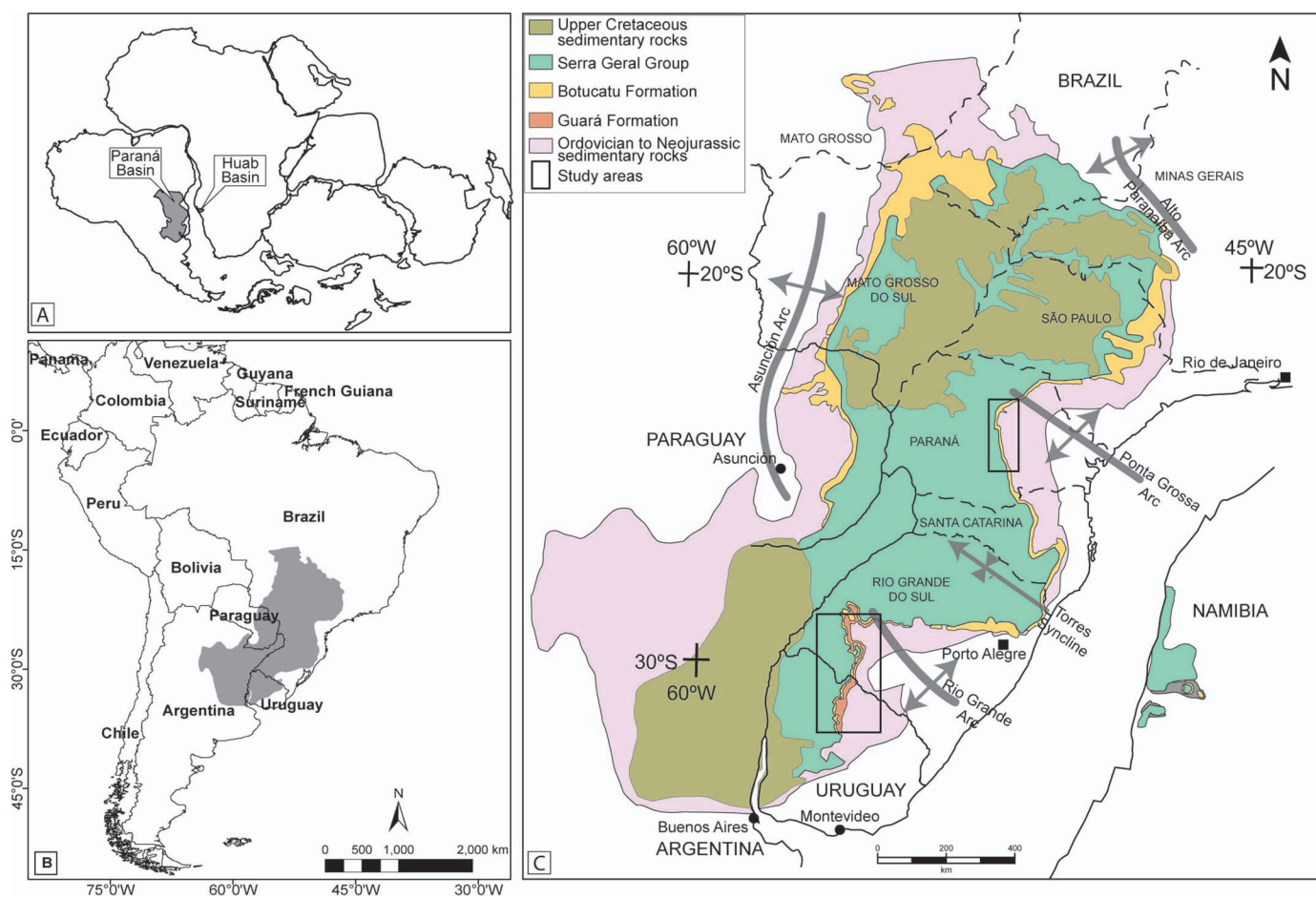


FIG. 1.—Location of the study areas in Paraná Basin and Gondwana contexts. A) Paraná Basin and its counterpart Huab Basin in southwestern Africa, positioned in Late Jurassic Gondwana, based on the Schmitt and Romeiro (2017) reconstruction. B) Position of the Paraná Basin in South America. C) Map of the Paraná Basin showing the study areas (modified from Zalán et al. 1987; Scherer and Lavina 2005, 2006; Scherer and Goldberg 2007; Rossetti et al. 2017; Amarante et al. 2019).

Amarante et al. (2019) and Reis et al. (2019) suggest that the Jurassic Guará Formation of Brazil and the genetically correlative Batoví Member of Uruguay represent deposits of a large distributive fluvial system that flowed from NE to SW (Fig. 1) for at least 1050 km in the Paraná Basin in southwestern Gondwana. This study quantifies the characteristics of fluvial facies and architecture of the Guará Formation–Batoví Member along a downstream-oriented transect in order to refine a large-scale depositional model for the formation and to verify whether the formation-scale depositional model matches those established for DFSs. In addition, this study confidently reports the identification of the largest distributive fluvial systems recognized from both modern and ancient datasets. In comparison with other quantified DFSs in the literature (Hirst 1991; Owen et al. 2015; Wang and Plink-Björklund 2019), this study also provides insights into depositional dynamics at the DFS distal termination, where the system interacted with aeolian systems, such as those provided at a facies level by Cain and Mountney (2009). This work therefore aims to test the hypothesis that DFSs may dominate the continental stratigraphic record through quantitative analysis of an Upper Jurassic succession exposed across southern Brazil and northern Uruguay.

Given the great spatial extent of the distributive fluvial system reconstructed here, this study also provides data that can be used to integrate paleogeographic and paleoclimatic reconstructions of western Gondwana during the Late Jurassic. Few studies focus on facies and stratigraphic characterization of Late Jurassic units in the region (Mountney et al. 1998; Veiga and Spalletti 2007; Francischini et al.

2015; Linol et al. 2015), despite this time interval being critical in understanding paleoenvironmental, paleoclimatic, and geotectonic changes related to Gondwana fragmentation, a critical time period in Earth's history. The breakup of western Gondwana, together with the evolution of the Paraná–Etendeka plume, controlled erosion and sedimentation in the Mesozoic Era (Friedrich et al. 2018; Krob et al. 2020). This study therefore rectifies this knowledge gap through quantitative analysis of the Guará Formation–Batoví Member across a large part of the Paraná Basin, recording climate and paleogeography of southwestern Gondwana in the Late Jurassic (Scherer and Lavina 2005, 2006; Perea et al. 2009; Amarante et al. 2019; Reis et al. 2019). The quantitative analysis of the Guará Formation provides robust documentation of sedimentary-basin fill in a significant geological time period in relation to continental-crust evolution over an active plume.

We also test how readily DFS deposits can be recognized without large-scale outcrop belts, such as those exposed across the southwestern USA (Owen et al. 2015, 2019; Wang and Plink-Björklund 2019) and Spain (Hirst 1991). The study was conducted by extracting information from smaller-scale outcrops (typically 5–15 m high) analyzed in the context gained from key medium-scale-exposure outcrops (20–50 m high), and integrated by information from available well cores. Relatively limited, sparse datasets are the reality of geology work in larger parts of continental basins, and therefore it is important to test the applicability of DFS facies models also with such datasets (i.e., where the outcrops are extremely weathered and covered by vegetation for good parts of the basin).

		SW Uruguay (from Perea et al., 2009)	Rio Grande do Sul State (western block), Brazil (from Scherer et al., 2021)	NE Paraná State, Brazil (modified from Milani et al., 2007; Reis et al., 2019; Christofoletti et al. 2021)
Cretaceous	Upper			Bauru Gr.
	Lower	Arapey Fm. Rivera Mb.	Serra Geral Gr. Botucatu Fm.	Serra Geral Gr. Botucatu Fm.
Jurassic	Upper	Tacuarembó Fm. Batoví Mb.	Guará Fm.	Guará Fm.
	Middle			Pirambóia Fm.
	Lower		Mata Sandstone Caturrita Fm. Santa Maria Fm. Sanga do Cabral Fm.	
Triassic	Upper			
	Middle			
	Lower			
Permian	Buena Vista Fm.	Buena Vista Fm. / Rio do Rasto Fm.	Rio do Rasto Fm.	

FIG. 2.—Summary of lithostratigraphic units of the Paraná Basin. Modified from Reis et al. (2019) after Soares (1975), Milani (1997), Scherer et al. (2000, 2021), Milani et al. (2007), Perea et al. (2009), and Christofoletti et al. (2021). SW, southwest; NE, northeast; Gr., Group; Fm., Formation; Mb., Member.

GEOLOGICAL SETTING

The Paraná Basin is an intracratonic basin covering an area of 1,400,000 km² across Brazil, Argentina, Uruguay, and Paraguay, with a small remnant eastern part preserved as the Huab Basin of Namibia (Milani et al. 2007) (Fig. 1). The basin records various phases of subsidence and sedimentation from the Ordovician to the Cretaceous (Milani 1997; Milani et al. 1998, 2007) (Fig. 2). The Upper Jurassic Guará Formation is bounded by unconformities at the base and top, defining a distinct depositional sequence in the Paraná Basin (Scherer et al. 2000, 2021) (Fig. 2). The thickness of the Guará Formation ranges from 12 to 110 m in Brazil, cropping out in the Paraná and the Rio Grande do Sul states (Scherer and Lavina 2005, 2006; Reis et al. 2019). In Uruguay, this lithostratigraphic unit is equivalent to the Batoví Member of Tacuarembó Formation (Fig. 2), which can be up to 200 m thick (Amarante et al. 2019). In Brazil, the Guará Formation unconformably overlies the fluvial–aeolian deposits of the Pirambóia Formation in the Paraná State and the Sanga do Cabral Formation in the Rio Grande do Sul State (Scherer et al. 2000; Reis et al. 2019), while the Batoví Member in Uruguay unconformably overlies aeolian deposits of the Buena Vista Formation (Amarante et al. 2019) (Fig. 2). In both countries, the Guará Formation and Batoví Member are unconformably overlain by the aeolian deposits of the Lower Cretaceous Botucatu Formation (Brazil) and Rivera Member (Uruguay), respectively (Scherer et al. 2000, 2021; Scherer and Lavina 2005, 2006; Amarante et al. 2019; Reis et al. 2019) (Fig. 2).

The Guará Formation–Batoví Member is composed of fine- to coarse-grained sandstones and rare mudstones (Scherer et al. 2000; Scherer and Lavina 2005, 2006; Perea et al. 2009; Amarante et al. 2019; Reis et al. 2019), with internal facies zonation. The northern part (Paraná State and the northern Rio Grande do Sul State) is composed of coarse- to medium-grained sandstones deposited by braided fluvial systems that transition southwards to medium- to fine-grained sandstones, deposited by fluvial channels, distal terminal channels and unconfined runoff, aeolian dunes, and aeolian sand sheets (southern Rio Grande do Sul State and Uruguay).

Paleocurrents from aeolian dunes indicate a NE migration direction, while fluvial systems flowed towards the SSW (Scherer and Lavina 2005; Amarante et al. 2019; Reis et al. 2019).

The Guará Formation in the western region of Rio Grande do Sul State, Brazil, was first recognized by Scherer and Lavina (2005) as a continental sedimentary succession with a dominance of fluvial deposits in the proximal region and fluvial–aeolian wetting-upward cycles in the more distal regions. Paleocurrents obtained from aeolian-dune cross strata were to the NE, and the fluvial paleocurrents were to the SSW (Scherer and Lavina 2005). Reis (2016) interpreted fluvial deposits of the Guará Formation as alternations of perennial and ephemeral fluvial channel deposits controlled by climatic variations. Perea et al. (2009) correlated the fluvial–aeolian succession of the Batoví Member (lower part of Tacuarembó Formation) in northwestern Uruguay with the Brazilian Guará Formation. A Late Jurassic–Early Cretaceous age was attributed to the unit based on the rich fossil content (Perea et al. 2009). Later, Amarante et al. (2019) detailed the stratigraphy of the Batoví Member, interpreting five facies associations (aeolian dunes, aeolian sandsheets, ephemeral fluvial channels, perennial braided fluvial channels, and distal sheetfloods) to suggest they composed the record of the distal part of a distributive fluvial system. The Guará Formation was recognized in its northernmost part by Reis et al. (2019), specifically in Paraná State in Brazil, the northwestern border of the Paraná Basin. Reis et al. (2019) distinguished the contacts of the Guará Formation from underlying and overlying units by means of unconformities which may represent depositional hiatuses associated with significant climatic changes. In Paraná State, the Guará Formation consists of multistory perennial fluvial channel fills with a consistent paleocurrent pattern to the SW (Reis et al. 2019). The depositional characteristics (detrital composition, sedimentary processes, paleocurrent pattern, stratigraphic framework) compared between the entire Guará Formation NE–SW outcrop belt (from Paraná State, Brazil, to Uruguay) demonstrated downstream reduction in grain size and changes in facies-association proportions reinforced the DFS interpretation suggested by Amarante et al. (2019). Reis et al. (2019) also suggested that the large

DFS interpreted for the Guará Formation may be linked, between other Late Jurassic depositional sites, to the breakup of Gondwana and the opening of the southern Atlantic Ocean.

A diverse fossil content is present in the Guará Formation–Batoví Member, with body-part preservation of crocodilians, turtles, sauropods, ornithopods, theropods, megalosaurs, pterosaurs, sharks, lungfishes, coelacanths, mollusks, and conchostrachans (Mones 1980; Martínez et al. 1993; Perea et al. 2001, 2003, 2009, 2014, 2018; Yanbin et al. 2004; Soto and Perea 2008, 2010; Fortier et al. 2011; Soto et al. 2012a, 2012b, 2020), as well as dinosaur ichnofossils (Dentzien-Dias et al. 2008; Francischini et al. 2015, 2017; Mesa and Perea 2015). Paleoecologic interpretations confirm a fluvial environment established in a continental semiarid to arid climatic regime. Perea et al. (2009) performed an extensive biostratigraphic revision restricting the age of the Batoví Member to not older than Kimmeridgian (Late Jurassic) and not younger than Hauterivian (Early Cretaceous). Comparison of dinosaur ichnofaunas of the Guará Formation to those of the Botucatu Formation (Early Cretaceous) (Francischini et al. 2015, 2017) demonstrate reduction in body size and a disappearance of taxa between the two units. Francischini et al. (2015) attribute these discrepancies to a hiatus in deposition between Late Jurassic and Early Cretaceous, associated with significant aridification. A detailed biostratigraphic revision established the theropod genus *Ceratosaurus* as a fossil index to the Kimmeridgian–Tithonian age of the Guará Formation–Batoví Member (Soto et al. 2020).

METHODS AND DATASET

Data were collected through the construction of graphic sedimentary logs, considering the characteristics of facies and bounding surfaces. In total, 1,071.2 m of stratigraphy were logged across 62 outcrop locations and 2 wells. The location distribution follows the general NNE–SSW outcrop-belt orientation (see Paleoflow subsection of Spatial Analysis Results). The same group of lithofacies was identified both in outcrops and well-core descriptions. Sedimentary logs were interpreted through classic methods of facies analysis, where groups of genetically related facies are categorized into facies associations that represent deposits of sub-environments that compose the depositional systems (Walker and James 1992). Facies associations with defined morphology were classified as architectural elements, especially for fluvial deposits (Miall 1985; James and Dalrymple 2010).

Both well and outcrop data were input into a digital database and classified by facies code, bed thickness, grain size, architectural element, and facies association. Grain size was measured on the Wentworth millimetric scale, then converted to the phi scale to avoid statistical bias caused by magnitude differences between grain-size classes in the millimetric scale. To account for channel-body thickness, the weighted average of the phi grain size was used herein (following Owen et al. 2015).

To ensure representative “snapshots” at the system scale (i.e., using outcrop sections of adequate thickness in relation to the total thickness of the formation), exposures that were below 25% of the total formation thickness were discounted from statistical analysis. The cutoff value was chosen based on measured channel-body thickness. From the original dataset, this left 17 locations that total 718.9 m of stratigraphy (67.11% of total data logged). Sections whose thickness measured less than 25% of the total formation thickness were considered only for paleocurrent insights. The estimates of facies-association proportions presented here are derived from relative abundances along these 17 representative logged sections.

Presence and strength of observed trends were identified using the (non-parametric) Spearman’s rank correlation coefficient (R_s). Where $R_s = 1$, a perfect positive correlation exists, and where $R_s = -1$, a perfect negative correlation exists, while R_s values near 0 indicate that the two factors are independent (i.e., there is no correlation) (Davis 2002). A null hypothesis (H_0) of absence of correlation between variables was established, and

critical probability values (p values) were calculated in order to measure the probability of any observed correlation to be due to chance. Higher p values (close to 1) suggest minimal evidence of rejecting the null hypothesis, indicating absence of correlation, while very low p values (close to zero) constitute strong evidence of rejection of the null hypothesis, and acceptance of the alternative hypothesis (H_1) that there is correlation between the studied variables. A frequently used significance level of 5% was used ($\alpha = 0.05$) for the calculated p values, under which the null hypothesis was rejected. Due to small sample size ($n \approx 17$), only R_s correlation coefficients above critical values for certain sample sizes (taken from the widely available Spearman’s rank significance table at a level of 5%) were taken into account. Spearman’s correlation was performed using R software, a widely used open-source statistical platform. Mean paleocurrent directions were mapped for deposits of both perennial and ephemeral fluvial channels, as well as for aeolian-dune strata.

RESULTS

Facies and Facies Associations

Sandstones of the Guará Formation range in grain size from fine- to very coarse-grained sandstones through to gravelly sandstones (and associated conglomerates) (Table 1). Fluvial facies range from moderately to very poorly sorted, dominantly poorly sorted, with subrounded to rounded grains. In aeolian facies, sandstones are fine- to medium-grained, well-sorted, and well rounded. The gravel fraction varies from rounded to subangular—typically quartz clasts are more rounded while mud clasts and lithoclasts are subrounded to subangular. The sandstones and conglomerates of the Guará Formation are compositionally very homogeneous. Sand fractions are classified as quartzarenites, while the gravel fraction is composed of quartz (granules to pebbles), mud clasts (granules to boulders), and sedimentary lithoclasts (pebbles to boulders). The presence of sedimentary lithoclasts is notable in gravel fractions, as it is composed of fine- to medium-grained sandstone clasts varying from pebble to boulder size classes, and granule- to boulder-size mud clasts. Fine sediments occur as mudstones, siltstones, very fine-grained sandstones, and rarely claystones, frequently associated with heterolithic bedding.

Three main facies associations were determined: fluvial channel fills, floodplain, and aeolian deposits (Fig. 3). The fluvial channel fills are subdivided into two types: perennial and ephemeral (Fig. 3), following the hydrology-based classification by (Fielding et al. 2018). The floodplain facies association encompasses alluvial sediments accumulated outside main channels, including muddy floodplain, crevasse splays, crevasse channel fills, and terminal sheetflood deposits (Fig. 3). The aeolian facies association includes deposits of aeolian dunes, interdunes, and aeolian sand sheets (Fig. 3). The main features of architectural elements are summarized in Figure 4.

A bounding-surface hierarchy was established, adapted from Miall (1988) and Owen et al. (2017). The limits between architectural elements are equivalent to the Miall (1988) fourth-order surface and Owen et al. (2017) barform surface. Story surfaces (corresponding to fifth-order surface of Miall 1988) are erosional and represent the incision and establishment of an active channel into previous deposits, later infilled by one or more architectural elements. The amalgamation of two or more stories builds up a multi-story channel body, in opposition to single-story channel bodies. The surface between a channel body and a non-channel element (floodplain or aeolian, in this study) corresponds to a sixth-order surface of Miall’s (1988) classification.

Perennial Fluvial Deposits

Description.—Channel bodies range from 1.2 to 15.3 m thick. The deposits are composed predominantly of trough (St, 81.2%) and planar (Sp, 8.6%) cross-strata (Fig. 3). Around 7% of total facies described are

TABLE 1.—Summary of lithofacies observed in Guará Formation (based on Scherer and Lavina (2005), Amarante et al. (2019), Reis et al. (2019), and data collected in this study).

Code	Description	Interpretation
Gm	Clast-supported sandy conglomerate, pebble-size quartz clasts, reddish muddy intraclasts and sandstone lithoclasts cobble to boulder-size, massive. The sandy fraction varies from fine- to very coarse-grained. Frequently at the base of cross-strata sets. Resting on erosion surfaces, filling scour.	Deposition of bedload as diffuse gravel sheets (Hein and Walker 1977) in the channel bottom, resulting from hyperconcentrated flows eroding previous gravelly sands (quartz pebbles), overbank deposits (mud clasts), and ancient sedimentary rocks (sandstone lithoclasts).
Gh	Clast-supported conglomerate, quartz pebbles, crudely horizontally bedded	Migration of longitudinal gravel bars in unidirectional flow (Miall 1996; Todd 1996).
Gt	Clast-supported sandy conglomerate, quartz pebbles, trough cross-bedded. Green muddy cobbles at the set base.	Migration of subaqueous sinuous-crested gravel dunes in unidirectional flow (Todd 1996).
Sm	Fine- to very coarse-grained sandstone, poorly to well-sorted, massive. Muddy pebbles at the base of the bed.	Fast deposition of subaqueous unidirectional high-energy flow, hyperconcentrated (Scherer et al. 2015) in sediments, fluidization or intensive bioturbation (Miall 1978, 1996).
Sh	Fine- to coarse-grained sandstones; well- to poorly-sorted, horizontal lamination.	Horizontally bedded deposits originated via unidirectional supercritical flow (Miall 1978; Bridge and Best 1988).
Sl	Fine to coarse-grained sandstone, moderately to poorly sorted, low-angle cross stratification. Quartz and muddy granules and pebbles dispersive, mark stratification and base of beds.	Structures formed in transitional flow between subcritical and supercritical (Harms et al. 1982; Bridge and Best 1988).
Ss	Fine- to very coarse-grained, moderately sorted sandstone with sigmoidal cross stratification.	Migration of subaqueous dunes with rapid aggradation combining traction and suspension in lower- to upper-flow regime (Wizevich 1992).
St	Fine- to very coarse-grained, well- to poorly- sorted gravelly sandstone, trough cross-stratified. Foresets and sets are normal graded. Quartz and muddy granules and pebbles dispersive, at the set base and marking the foresets. Frequently deposited above Gm facies bed.	Migration of subaqueous sinuous-crested dunes in unidirectional flow (Allen 1963; Miall 1978; Collinson et al. 2006).
Sp	Fine to coarse-grained, moderately to poorly sorted sandstone, planar cross-stratified. Foresets and sets are normal graded. Dispersed quartz granules. Mudclasts and quartz granules and pebbles at the set base.	Migration of subaqueous straight-crested dunes in unidirectional flow (Allen 1963; Miall 1977; Collinson et al. 2006).
Sr	Very fine- to coarse-grained, moderately to well-sorted sandstone with ripple cross-lamination, subcritical to supercritical climbing angle.	Migration of unidirectional subaqueous 2-D or 3-D ripples in lower flow regime (Allen 1963; Miall 1977).
Sd	Fine- to medium-grained sandstones with deformed undefined lamination; occasionally containing mudclasts.	Deformation of primary structures by liquefaction in unconsolidated layers (Owen and Moretti 2011).
S	Fine- to very coarse-grained sandstones in which it is not possible to recognize the primary structure.	Sandstones with structures obliterated by diagenetic or weathering action.
Ht	Millimetric to centimetric heterolithic lenticular to flaser bedding; intercalations of very fine to fine sandstones (massive, sometimes with ripples), mudstones, claystones, and siltstones, laminated or massive; commonly presenting bioturbation and plastic-deformation structures, which breaks the lamination.	Deposition by decantation of suspended load alternating with bed load or rapid deposition of hyperpycnal flow in a flow regime very close to zero. Plastic deformation due to fluidization and overloading (Amarante et al. 2019).
Fl /Fd	Mudstones (claystones, siltstones, and very fine-grained sandstones), with millimeter-size horizontal lamination. Structures of plastic deformation are common, breaking lamination (facies Fd). Gray, purple, red to reddish-brown. Mottling, blocky cleavage and root marks occur occasionally.	Deposition of suspended load by settling in standing water (Miall 1977; Turner 1980; Jo and Chough 2001). Purple, red and brown colors associated with mottling, blocky cleavage, and root marks indicate pedogenic alteration (Retallack 1988).
Fm	Mudstones to (claystones, siltstones, and very fine-grained sandstones), massive; sometimes fissile in weathered surfaces. Gray, purple, red to reddish-brown. Mottling, blocky cleavage and root marks occur occasionally.	Deposition of suspended load by settling in standing water (Miall 1977; Turner 1980; Jo and Chough 2001). Lack of lamination due to i) flocculation of clay suspension, or ii) loss of lamination associated with fluidization or intense bioturbation. Purple, red, and brown colors associated with mottling, blocky cleavage, and root marks indicate pedogenic alteration (Retallack 1988).
Sl(e)/Sh(e)	Fine- to medium-grained sandstones, well-sorted, with well-rounded and highly spherical grains, horizontal to low-angle lamination formed by thin pinstripe inversely graded laminae.	Translatent subcritical wind ripple migration over a plane to quasi-plane surface (Kocurek 1981).
St(e)	Fine- to medium-grained sandstones, well-sorted, with well-rounded and highly spherical grains, large-scale trough cross-bedding. The base of the foresets consists of millimetrically spaced pinstripe laminations with inverse grading, which interdigitates with wedges of massive sandstones up to 4 cm thick towards the top of the foresets; frequent presence of reactivation surfaces.	Sinuous-crested (3-D) aeolian dunes alternating grainflow and translatent subcritical wind-ripple migration in the lee side (Hunter 1977; Hunter and Rubin 1983).
Sa(e)	Dominantly fine-grained sandstone, rarely medium-grained, well-sorted, with crenulated plane-parallel lamination, defining a crinkled texture.	Adhesion structures originating from adherence of dry sand grains that were carried by wind over wet surfaces (Kocurek 1981; Kocurek and Fielder 1982).

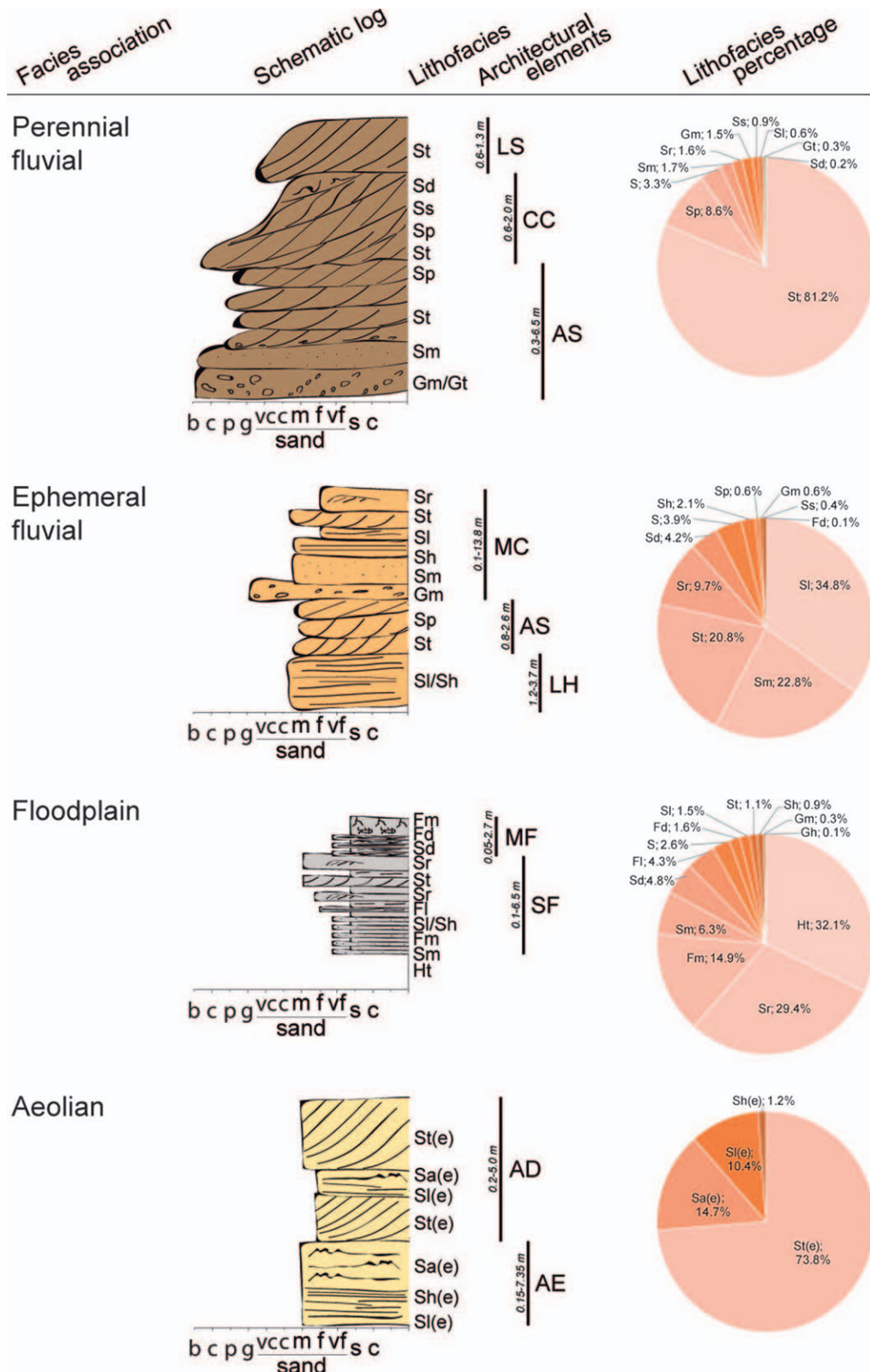


FIG. 3.—Schematic logs of facies associations, architectural elements, and respective facies distributions. LS, large simple cross-bed sets; CC, downcurrent-dipping compound coset; AS, amalgamated cross-bedded sets; MC, massive to cross-bedded sand sheets; LH, low-angle to horizontally stratified sand sheets; MF, muddy floodplain deposits; SF, sandy floodplain deposits; AD, aeolian dunes and interdunes; AE, aeolian sand sheets.

Architectural Element	Constituent Facies	Interpretation	Illustration	e.g.
Large simple cross-bed sets (LS)	Sp and St	Migration of unit bars		Figure 6
Downcurrent-dipping compound coset (CC)	St and Sp	Migration of compound unit bars		Figure 5A
Amalgamated cross-bedded sets (AS)	St, Sp and rarely Ss	Migration and climbing of individual subaqueous dunes accumulated by vertical aggradation		Figure 5A
Low-angle to horizontally stratified sand sheets (LH)	Sl and Sh	Sand sheets deposited by transcritical- to upper-flow-regime		Figure 5A
Massive to cross-bedded sand sheets (MC)	Gm, Sm, Sh, Sl, St and Sr	Deposition by waning flows, representative of multi-episodic channel fill under settings with ephemeral and intermediate discharge variability		Figure 5A
Sandy floodplain deposits (SF)	Sr, Sm, or Sl, St, Sh alternated with Fm and Fl beds. Rarely Gm	Unconfined flows outside of main fluvial channels (e.g., crevasse channels and splays, and terminal splays)		Figure 5A
Muddy floodplain deposits (MF)	Ht and Fl	Decantation of fine-grained sediments in floodplains after bankfull events		Figure 5B, 5C and 6
Aeolian dunes and interdunes (AD)	St(e), Sa(e) and Sl(e)	Progradation and aggradation of 3D crescentic aeolian dunes. Wet and dry interdunes occur interbedded with dune deposits		Figure 5D, 5E
Aeolian sand sheets (AE)	Sl(e) and Sa(e)	Sand sheets deposits with adhesion structures and low-angle wind-ripple lamination		Figure 5E

FIG. 4.—Summary of architectural elements detailing lithofacies composition, geometry, and interpretation.

distributed in massive (Sm, 1.7%) and ripple cross-laminated (Sr, 1.6%) sandstones, thin beds of massive conglomerates with mud clasts (Gm, 1.5%), sigmoidal cross-bedded sets (Ss, 0.9%), low-angle cross-stratified (Sl, 0.6%) sandstones, trough cross-stratified conglomerates (Gt, 0.3%), and sandstones bearing secondary deformation structures (Sd, 0.2%) (Fig. 3). For the remaining 3.3% of the facies described, it was impossible to identify primary structures (S) (Fig. 3). Story successions from 0.5 to 9.5 m thick are characterized by poorly defined fining-upward facies successions bounded at the base by undulated to concave-up surfaces that are commonly lined by gravelly facies (Gm and Gt). Architectural elements of perennial fluvial deposits are identified based on facies and deposit geometry, being namely: large, simple cross-bed sets, down-current-dipping compound cosets, and amalgamated cross-bedded sets (Fig. 4) as follows:

- Large simple cross-bed sets (LS): Isolated, planar or tangential cross-stratified sets (Sp and St) varying from 0.6 to 1.3 m thick, with an average thickness of 0.8 m, extending laterally up to 20 m (limited to outcrop extent). Frequently the foresets are truncated by regularly spaced (0.15 to 0.20 m) concave-up, convex-up, or concave-to-convex (sigmoidal) erosion surfaces, overlain by downlapping foresets.
- Downcurrent-dipping compound coset (CC): Cross-stratified sets (facies St and Sp), 0.10–0.25 m thick, bounded by surfaces dipping in the same direction of cross-bedding foresets, but at a shallower angle (4–20°). The compound cosets are 0.6 to 2.0 m thick, with average thickness of 1.2 m. Individual foresets and sets are frequently normally graded.
- Amalgamated cross-bedded sets (AS): Cross-stratified sets (St, Sp, and rarely Ss) with average thickness of 0.20 m, ranging from 0.10 to 0.50 m, amalgamated in tabular packages from 0.3 to 6.5 m thick, with average thickness of 1.9 m, and extending laterally for tens of meters in packages underlain by erosion surfaces. The boundaries between sets are undulated to concave-up in sections transverse or oblique to the paleoflow. In sections parallel to paleoflow, set boundaries tend to be slightly undulating to gently inclined in a direction opposite to paleoflow (cross-bedding foresets). Normal grading is common in foresets and sets.

Interpretation.—Amalgamated, poorly defined, fining-upward facies successions bounded by erosion surfaces and composed of poorly sorted and normally graded sandstones in cross-stratified medium- and large-scale sets are typical fluvial-channel deposits (Collinson 1996; Miall 1996). Large, simple cross-sets are interpreted as unit bars with a well-developed slipface (Wizevich 1993; Scherer et al. 2015; Amarante et al. 2019; Herbert et al. 2019). Cosets formed by sets dipping in the general paleocurrent direction typify compound unit bars where dunes superimposed over the bars migrated along the slightly inclined lee face of the bar (Scherer et al. 2015). The preservation of both simple and compound unit bars in the same channel fills indicates variations in discharge, depth, and continuity of flow through time (Herbert et al. 2019). Unit bars could represent mid-channel bars in small rivers or the mobile part of much larger and long-lived mid-channel bars in larger river channels (Herbert et al. 2019). Small amalgamated sets are interpreted as the product of migration and climbing of individual subaqueous dunes that accumulated by vertical aggradation, similar to the sand bedform element of (Miall 1985, 1996). These elements probably accumulated between mid-channel bars in the deepest parts of fluvial channels (Bristow 1987; Jo and Chough 2001). Migration of individual bedforms could also occur over the stoss side of mid-channel bars during bankfull stages (Miall 1996).

The close association of unit bars and subaqueous dunes suggests that the channels experienced a relatively low variability of interannual discharge (Fielding et al. 2018), implying a perennial channel interpretation by (Miall 1996). While the bedforms and macroforms suggest regularity in interannual discharge variations, the reactivation surfaces in

unit-bar deposits and the relatively broad range of preserved cross-bed (co)set thickness values could indicate a higher degree of discharge variability, possibly modulated by seasonality (Allen et al. 2014; Scherer et al. 2015; Fielding et al. 2018; Herbert et al. 2019).

Ephemeral Fluvial Deposits

Description.—This facies association is composed of tabular channel sand bodies between 0.25 and 12 m thick, and one anomalously thick (25.2 m) unit. The sand bodies represent multi-story or single-story channel fills. Stories vary in thickness from 0.25 to 4.75 m (with some outliers between 6.0 and 10.2 m), are bounded by sharp and erosion basal surfaces that are flat to concave-up, and can reach more than 1.5 m of relief. This facies association is composed of fine- to medium-grained sandstones and rarely fine mud-grade sediments. Beds of massive conglomerate (Gm) are common and occur along the basal erosional surfaces of stories. Almost 35% of the facies described in this association are sandstones with low-angle cross-stratification (Sl), 22.8% are represented by massive sandstones (Sm), 20.8% through cross-stratified sets (St), and 9.7% cross-laminated sandstones (Sr) (Fig. 3). Deformed sandstones (Sd) are more common (4.2%) than in perennial fluvial channel fills (Fig. 3). Horizontally stratified sandstones (Sh, 2.1%), planar cross-bedding (Sp, 0.6%), massive conglomerates (Gm, 0.6%), sigmoidal cross-bedded sandstones (Ss, 0.4%) and rare, deformed and discontinuous thin mudstone interbeds preserved between sandstone beds also occur (Fd, 0.1%; Fig. 3). Primary sedimentary structures were not recognizable in 3.9% of the sandstones (assigned to facies S). Each identified story comprises one or more architectural elements identified by their geometry and lithofacies assemblage: low-angle to horizontally stratified sand sheets, amalgamated cross-bedded sets, and massive to cross-bedded sand sheets (Fig. 4, 5A, 6) as follows:

- Low-angle to horizontally stratified sand sheets (LH): Tabular sandstone packages varying from 1.2 to 3.7 m thick (average thickness of 2.5) and up to 20 m of lateral extension, comprising almost exclusively low-angle (Sl) and horizontally (Sh) stratified sandstones. Rarely, cross-stratified bedsets (St) occur in isolated lenses. Quartz granules and pebbles are sparsely distributed within sandstone beds.
- Amalgamated cross-bed sets (AS): This element is similar to perennial fluvial deposits, but differs in size and geometry. In ephemeral channel fills, the individual cross-stratified bedsets (St, but sometimes Sp and Ss) are thinner (from 0.05–0.9 m thick, average thickness 0.23 m) and the architectural elements are less thick, stacked in tabular packages varying from 0.8 to 2.65 m (average thickness of 1.5 m), and extending for ~15 m.
- Massive to cross-bedded sand sheets (MC): This element is commonly composed, from base to top, of: massive intraformational conglomerates (Gm), massive sandstones (Sm), horizontally bedded and low-angle cross-stratified sandstones (Sh and Sl), trough cross-stratified sandstones (St), and ripple cross-laminated sandstones (Sr). The successions described consist of two or more of these facies, rarely all of them, while the stacking order remains consistent. These elements present well to poorly developed fining- and thinning-upward trends. Their external morphology can be tabular or lenticular, with sharp erosional concave-up bases. Average thickness is 2 m, ranging between 0.1 and 13.8 m, and lateral extent reaches up to 17 m (likely being underestimated due to the limited extent of available outcrops).

Interpretation.—The erosion bounding surfaces and the presence of unidirectional-flow structures indicate deposition in fluvial channels. Sand sheets formed by transcritcal-regime to upper-flow-regime sedimentary structures in alternation with amalgamated cross-stratified sets suggest a markedly variable discharge regime leading to within-channel accumulation under both subcritical and supercritical flow stages (Fielding et al. 2011, 2018; Allen et al. 2014). Alternatively, this facies alternation could

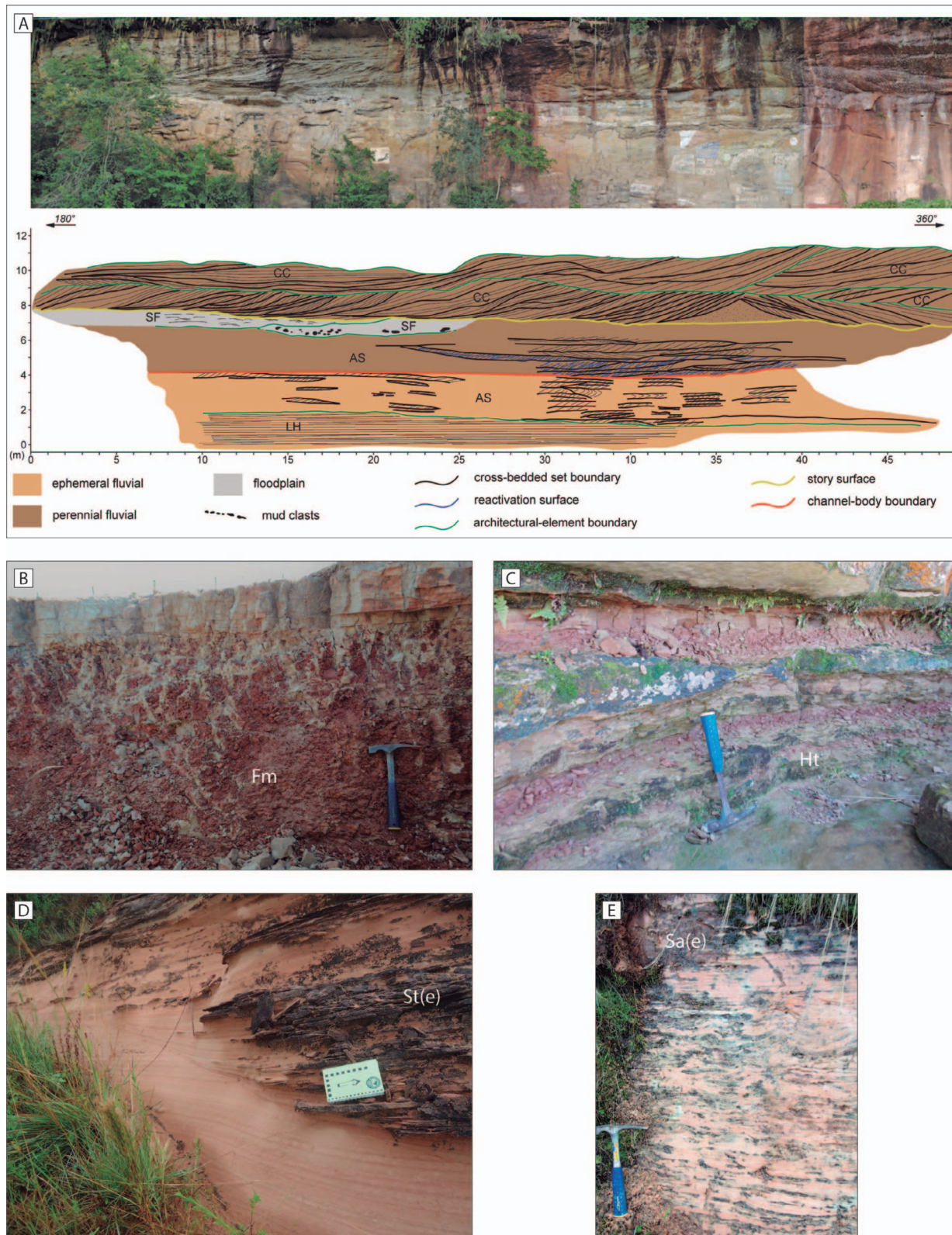


FIG. 5.—Examples of the facies associations. **A)** Interpreted panel showing the architectural elements of floodplain and fluvial channel deposits. Architectural elements: AS, amalgamated cross-bedded sets; LH, low-angle to horizontally stratified sand sheets; CC, downcurrent dipping compound coset; SF, sandy floodplain deposits. **B)** Muddy floodplain with pedogenic features. **C)** Thickening-upward heterolithic succession of the sandy floodplain. **D)** Large-scale trough cross stratification in aeolian-dune deposits. **E)** Adhesion structures in an aeolian sand-sheet deposit.

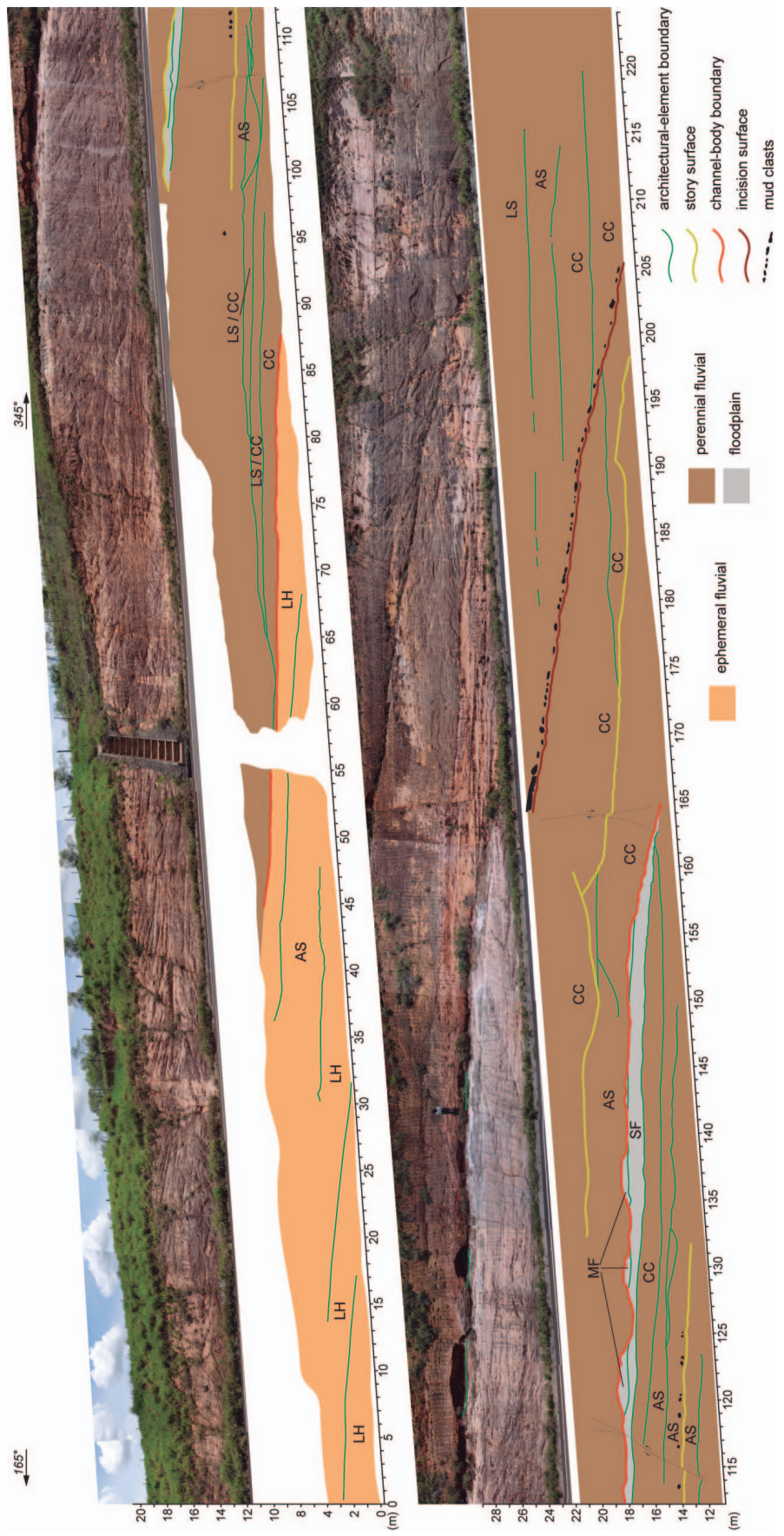


Fig. 6.—Interpreted lateral section of the GA002 outcrop, located \sim 700 km down-system. The architecture shows the characteristic amalgamation of fluvial channel bodies in the Guairá DFS. Architectural elements compose stories that are amalgamated in channel bodies. An ephemeral fluvial channel body was succeeded by the amalgamation of three perennial fluvial channel bodies. Floodplain deposits have highly eroded lenticular geometry. Note the high-relief erosion surface (red line) that truncates the entire channel-body package.

represent periods of slight flow confinement and migration of dunes followed by flow unconfinement generating transcritical structures (Bromley 1991). Facies successions representative of waning flows in sand bodies demonstrate the multiepisodic filling of a channel by successive flow episodes (Hampton and Horton 2007). The occurrence of massive sandstones indicates possible hyperconcentrated flows in which sediment concentration was particularly high, and/or flow deceleration too fast to allow bedform formation during final accumulation (Allen and Leeder 1980). The facies assemblage comprising dune elements, sand sheets with transcritical to supercritical structures, and facies successions indicating waning flow stages is characteristic for deposits of fluvial systems with intermediate discharge variability (Fielding et al. 2018) or affected by ephemeral discharge events (Scherer et al. 2007; Allen et al. 2014).

Floodplain Deposits

Description.—Deposits have tabular geometries that range in thickness from 0.2 up to 9 m (minimum lateral extent of 2.5 m, maximum extent limited by outcrop exposure). Sometimes the geometry is lenticular, due to erosional truncation by overlying channel fills (SF and MF elements, Figs. 5A, 6). The general facies distribution of these deposits is (Fig. 3): (Ht) Heterolithic bedding composed of massive or laminated mudstones thinly interbedded with fine or very fine massive or ripple cross-laminated sandstones (32.1%); (Sr) ripple cross-laminated, very fine to medium sandstones (29.4%); (Fm) massive mudstones (14.9%); (Sm) massive sandstones (6.3%); (Sd) sandstones bearing deformation structures (4.8%); and (Fl) laminated mudstones (4.3%). 6.1% of the facies are represented by sandstones with low-angle cross-stratification (Sl), with trough cross-stratification (St), horizontal bedding (Sh) and beds where primary structures are not identifiable (S). Deformed mudstones (Fd) constitute 1.6% of the identified facies. The remaining 0.4% are interpreted as massive and horizontally stratified conglomerates (Gm and Gh, respectively). This facies association is divided into two architectural elements, according to lithofacies features and sand/mud ratio: sandy floodplain deposits and muddy floodplain deposits (Fig. 4) as follows:

- Sandy floodplain deposits (SF): This element occurs as tabular packages that extend for tens of meters and are composed of sandstone beds with ripple cross-lamination (Sr), massive sandstones (Sm), or a variety of other sandstone facies (Sl, St, Sh) that alternate with massive and laminated mudstones (Fm and Fl) in beds of bedsets from millimeter to meter scale. Intraformational conglomerates (Gm) are rarely present. Lenticular geometries (0.5 m thick and 5–10 m long) are observed, always truncated at the top by erosion surfaces. This succession frequently shows thickening- and coarsening-upward trends of sandstone beds (Fig. 5C) in packages that range from 0.1 to 6.05 m thick (average thickness of 1.2 m).
- Muddy floodplain deposits (MF): This element has a lenticular geometry with a tabular base; however, its overall shape is controlled by subsequent erosion. Thickness ranges from 0.05 to 2.7 m (with an average of 0.5 m) in units that are generally discontinuous laterally but do not exceed 2 m. The alignment of non-eroded residual lenses over the same basal surface indicates that deposits may extend laterally up to 25 m. Deposits are composed predominantly of facies Ht and Fl, with frequently associated plastic-deformation structures (flame structures and convolute folding). Deposits are predominantly red and reddish-brown; however purple, brown, black, gray, and yellow colors are also present.

Interpretation.—The floodplain facies association consists of deposits representing deposition from mostly unconfined flows outside of main fluvial channels. Sandy intraformational conglomerates overlying erosion surfaces are interpreted as initial deposition in relatively proximal crevasses channels established onto floodplain fines (Donselaar et al. 2013). Tabular

and laterally continuous packages that alternate between mudstones and fine-grained sandstones with unidirectional tractive structures and lack of erosional features represent deposition from terminal splays. These deposits may represent the distal part of ephemeral channels or overbank flooding as a result of unconfined flows that overtapped adjacent channels (Hampton and Horton 2007; Scherer et al. 2015). Coarsening- and thickening-upward facies successions represent progradation of splay complexes developed downslope of, or lateral to, channel breaches (Morozova and Smith 1999; Spalletti and Piñol 2005; Hampton and Horton 2007). The muddy tabular deposits indicate floodplain deposition mainly by decantation of fines after bankfull events.

Aeolian Deposits

Description.—The basic lithology composing this facies association is fine- to coarse-grained sandstones with well-sorted and well-rounded quartz grains. Structures observed include small- to large-scale cross-bedded sets (St(e), 73.8%), corrugated and crenulated horizontal laminae (Sa(e), 14.7%) and low-angle and horizontal laminae (Sl(e) and Sh(e), 11.5%) (Figs. 3, 5D, E). The laminae are millimeters thick and well defined. This facies association is divided into two architectural elements: aeolian dunes and interdunes, and aeolian sand sheets (Fig. 4), as follows:

- Aeolian dunes and interdunes (AD): The cross-bedded sets (St(e)) are composed of grain-flow and wind-ripple laminae bounded by sharp and subhorizontal upper and lower surfaces. Individual sets range in thickness from 0.2 to 2.8 m (average of 0.9 m), with multiple sets forming tabular packages of up to 5 m thick. Tabular beds ranging from 0.1 to 1 m thick of crenulated horizontal lamination (Sa(e)) and low-angle lamination (Sl(e)) are sometimes identifiable between cross-bedded sets.
- Aeolian sand sheets (AE): Tabular packages with thickness ranging from 0.15 m to 7.35 m (average thickness 1.35 m) of low-angle to horizontal wind-ripple laminated sandstones (Sl(e)) and horizontal crenulated adhesion structures (Sa(e)). The limits between these facies are abrupt or gradational.

Interpretation.—Small-scale to large-scale trough cross-bedded sets composed of grain-flow and wind-ripple lamination are interpreted as the products of prograding and aggrading 3D crescentic aeolian dunes. The tabular bedsets preserved between dune cross-bedding and comprising horizontal crenulated adhesion structures or low-angle wind-ripple lamination represent deposition in, respectively, wet and dry interdunes (Mountney and Thompson 2002; Jones et al. 2016). The tabular packages composed of adhesion structures or low-angle wind-ripple lamination are interpreted as aeolian sand-sheet deposits (Fryberger et al. 1979; Scherer and Lavina 2005) when not interfingering aeolian dune-strata and overlaying sharp, planar surfaces.

Spatial Analysis

Paleoflow.—Paleocurrent data from fluvial channel sand bodies indicate a general flow direction SSW from the northern limit of the system in the Paraná State to Uruguay in the south (Fig. 7A, B, B1, C, C1, C2). This pattern indicates that the northern and southern outcrop belts (Fig. 7) are oriented sub-parallel to the dip direction of the entire system. Thereby, the outcrop-belt orientation provides insight into analysis of downstream spatial trends, over a great distance. Therefore, references to “distance downstream” here indicate the radial distance along a proximal-to-distal transect downsystem, measured from the northern occurrence of the Guará Formation (location PR011, Figs. 8, 9, 10B, 11E) to the SW, following the general paleocurrent pattern (Figs. 7, 8). In the broad SSW direction, local variations between west and southeast paleocurrents are identified and are attributed to frequent channel avulsion.

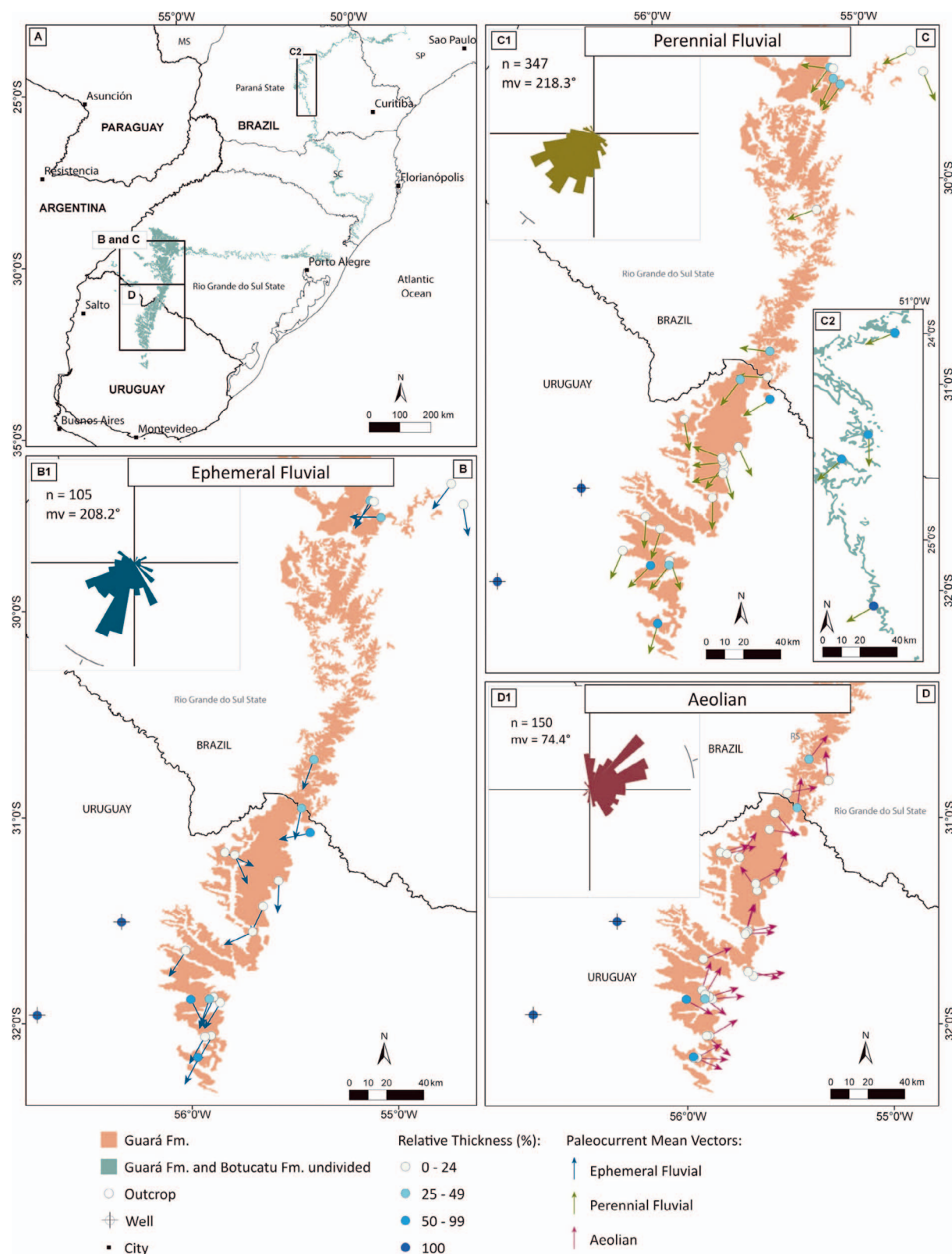


FIG. 7.—Maps of the paleocurrent distributions separated by facies associations. **A)** Location of the study areas. **B)** Ephemeral fluvial and **C)** perennial fluvial have similar paleocurrent dispersion, with mean vectors to the SSW (B1, C1). **D)** Aeolian paleocurrents are to the NE (D1).

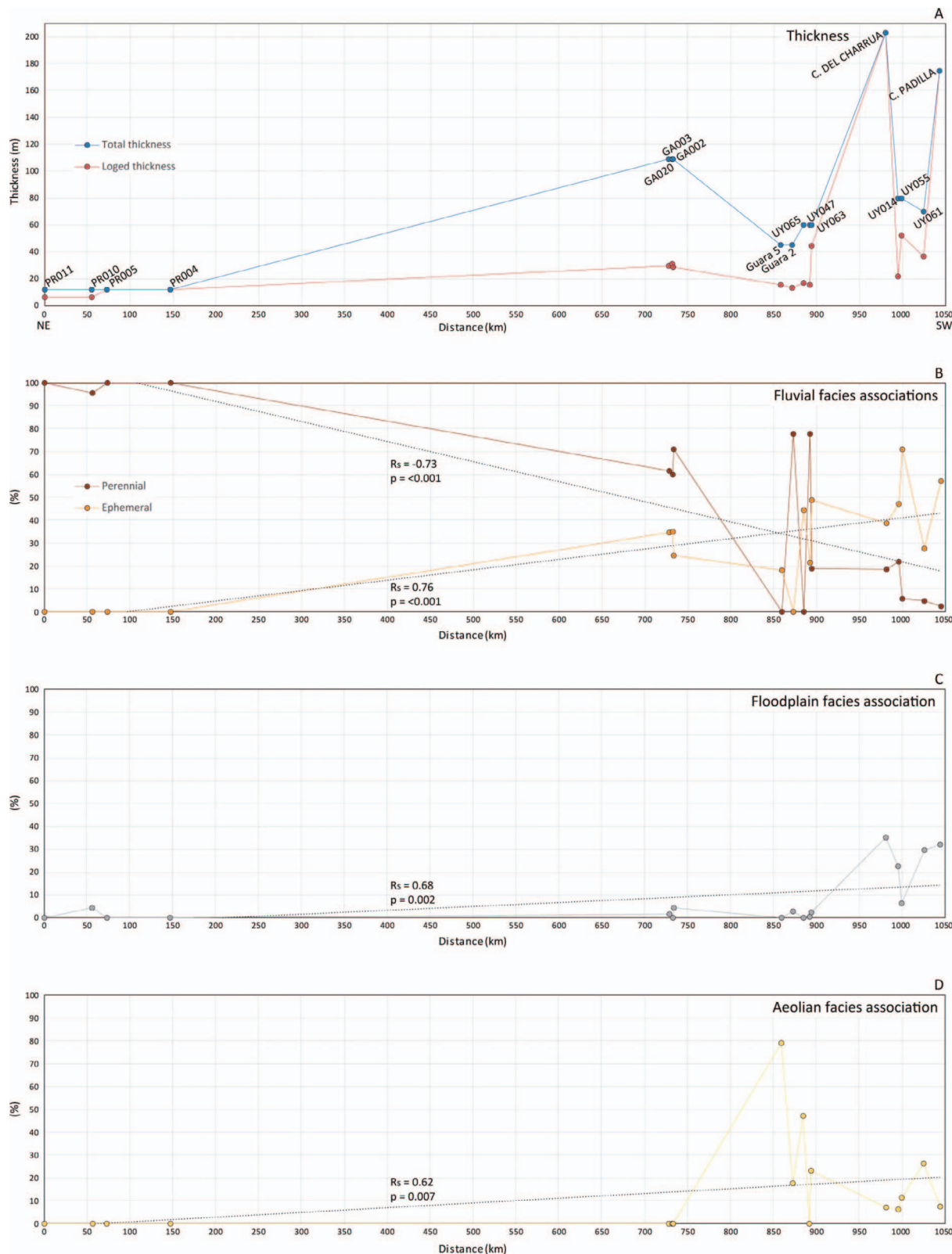


FIG. 8.—Spatial-analysis parameters plotted against downstream distance. **A)** Comparison between the thickness of the Guará Formation–Batoví Member and the thickness of each logged section used for quantitative analysis. **B)** Perennial versus ephemeral fluvial facies associations percentages. **C)** Floodplain facies association percentage. **D)** Aeolian facies association percentage.

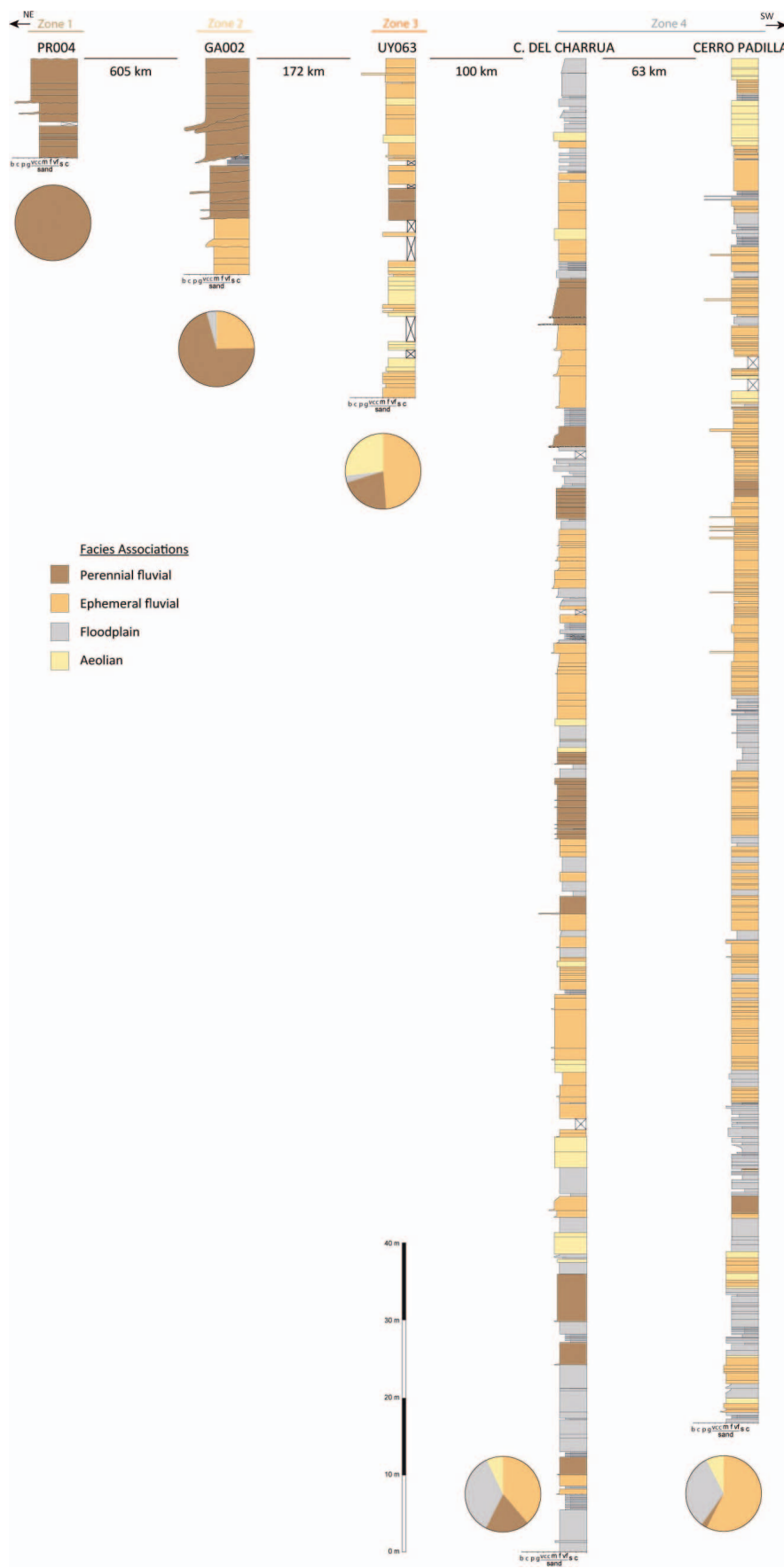


FIG. 9.—Selected logs exemplifying the lack of vertical stacking patterns of the Guará Formation. The pie charts show distribution of facies associations in each log. Location of the logs is in Figure 10.

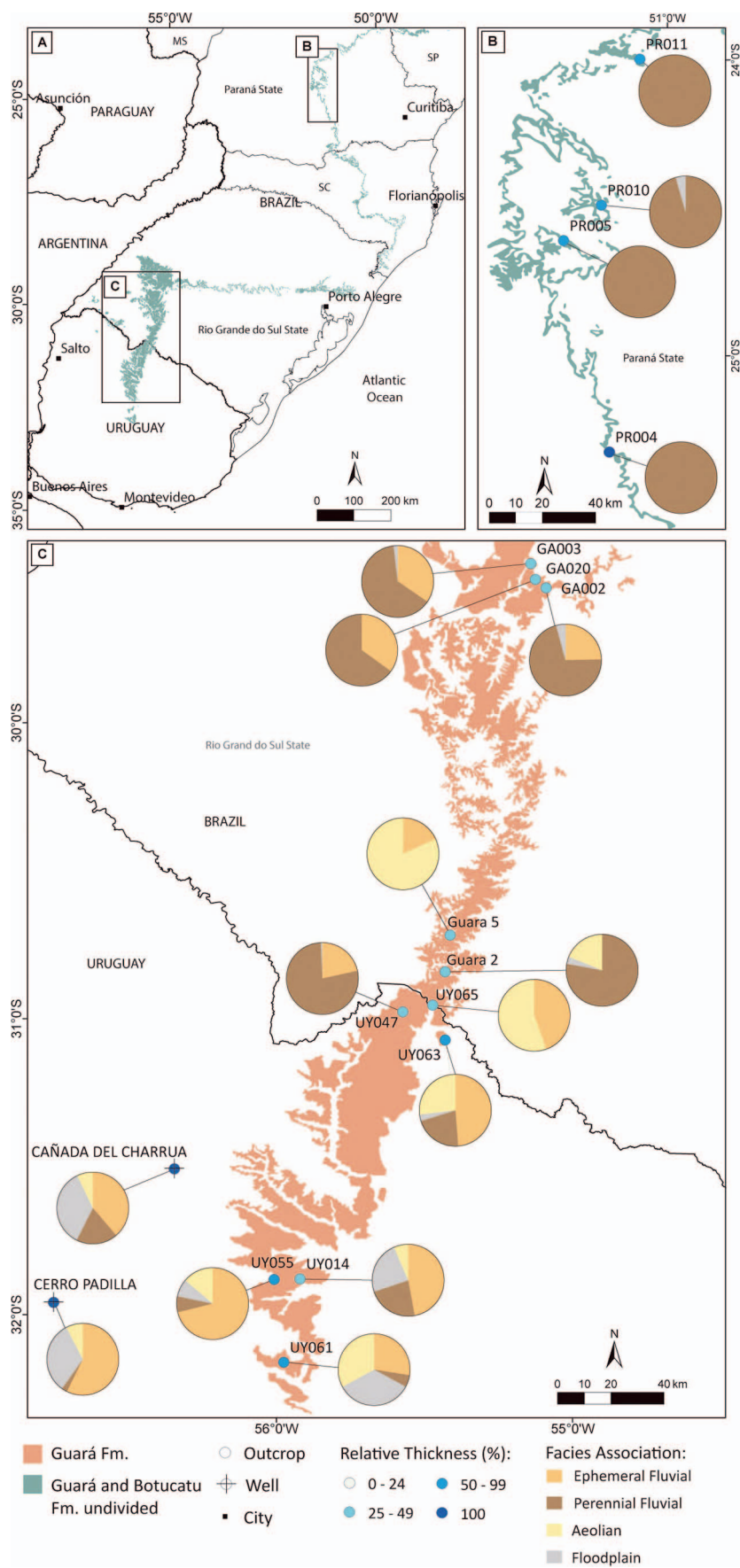


FIG. 10.—Distribution of facies-associations proportions. A) Location of the study areas. B) Paraná State area. C) Rio Grande do Sul and Uruguay area.

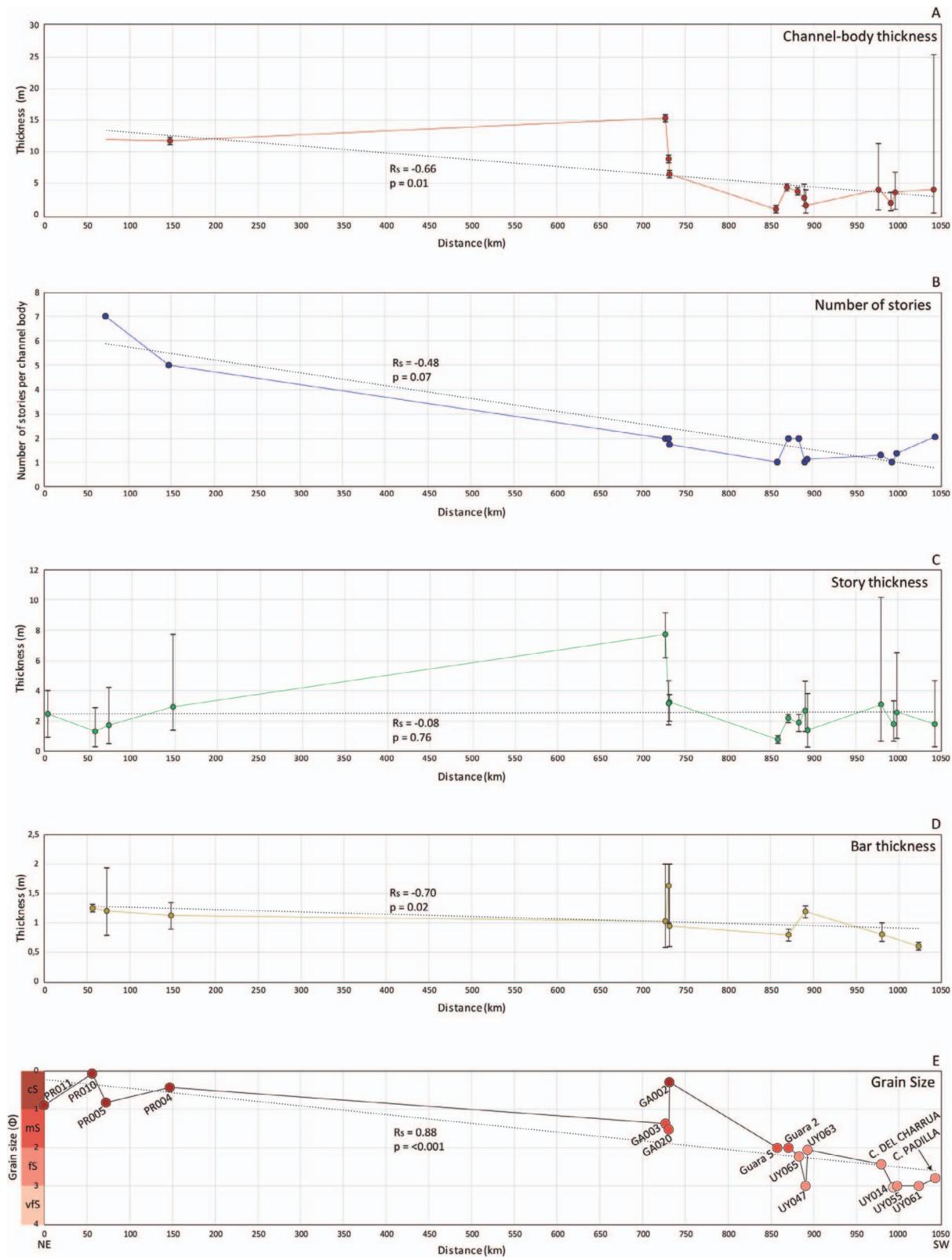


FIG. 11.—Fluvial features plotted against distance downstream. The error bars represent the variation between the maximum and minimum measure in each location. **A)** Channel-body thickness. **B)** Number of stories per channel body. **C)** Story thickness. **D)** Bar thickness. **E)** Weighted average grain size of the channel bodies.

TABLE 2.—Results of Spearman's rank correlation between observed parameters of the Guará Formation facies associations and distance downstream (n , number of observations; R_s , Spearman's coefficient of correlation; H_0 , null hypothesis at significance level $\alpha = 0.05$).

Parameter	n	R_s	p value	Evidence for Rejecting H_0	Correlation with Distance Downstream
% Perennial fluvial facies association	17	-0.73	< 0.001	very strong	strong, reliable
% Ephemeral fluvial facies association	17	0.76	< 0.001	very strong	strong, reliable
% Floodplain facies association	17	0.68	0.002	very strong	moderate, reliable
% Aeolian facies association	17	0.62	0.007	very strong	moderate, reliable
Channel-body thickness (average)	14	-0.66	0.01	strong	moderate, reliable
Number of stories per channel body (average)	14	-0.48	0.07	weak	weak, non-reliable
Story thickness (average)	16	-0.08	0.76	none	no correlation
Bar thickness (average)	10	-0.70	0.02	strong	strong, reliable
Grain size of fluvial channel fills (phi scale; weighted average)	17	0.88	< 0.001	very strong	strong, reliable

The distribution of aeolian paleocurrents shows a mean vector to the NE with a wide variability ranging over almost 180° (Fig. 7D, D1). This pattern confirms the model of westerly winds in mid-latitudes on the western margin of Gondwana in the Mesozoic (Scherer and Lavina 2006; Scherer and Goldberg 2007). The wide variation in the paleocurrent distribution of aeolian deposits is attributed to the crestline sinuosity of crescentic dunes.

Formation Thickness

The total thickness of the Guará Formation is variable across the region (Fig. 8A). Figure 8A shows the difference between the total formation thickness to the logged thickness in each location. The thinnest sections (around 12 m) are in the northeastern area (Paraná State), where the logged thickness closely approximates the total formation thickness. However, the total thickness varies both regionally and locally, as shown between wells (Cañada del Charrua, 202.30 m thick, and Cerro Padilla, 174.15 m thick) and in the outcrops closest to the wells (UY014, 80 m thick; UY055, 80 m thick; and UY061, 70 m thick) (Fig. 8A).

Stratigraphic Architecture

The Guará Formation shows downstream trends in architecture. In the northeastern region (Paraná State, relatively proximal), there is a high degree of amalgamation of channel fills of the perennial fluvial facies association (Fig. 9, log PR004). The central to southern part of the transect (Rio Grande do Sul State) is characterized by an alternation of perennial and ephemeral fluvial facies associations, still with a high degree of channel-fill amalgamation (Fig. 9, log GA002; Fig. 6). The degree of channel amalgamation decreases to the SW (relatively distal, according to the paleoflow), where the channel bodies are interbedded with aeolian and floodplain deposits (Fig. 9, logs UY065, Cañada del Charrua and Cerro Padilla). The vertical stacking pattern of facies associations does not present any cyclic correlation between the logs, contrary to suggestions by (Scherer and Lavina 2005) (Fig. 9).

A high-relief erosion surface cutting fluvial channel bodies is observed around 700 km downstream of the system, in the GA002 outcrop, Rio Grande do Sul State (Fig. 6). This surface is steeply dipping with more than 10 m of relief that truncates the channel bodies. Prominent mudstone boulders overlie the surface. In this location (GA002), the surface erosively truncates fluvial-channel fill deposits as well as is overlain by channel fill deposits of the same fluvial origin.

Proportions of Facies Associations

The proportions of facies associations vary along the NE–SW (downstream) dip-oriented transect. In the northeastern part of the study area (Paraná State), the perennial fluvial facies association dominates, ranging from 95 to 100% (Figs. 8B, 10B). Floodplain facies associations

constitute a minor proportion (5% in PR010) in this region. From 890 km downstream (near the Brazil–Uruguay border, UY047 log; Figs. 8B, 10C), the percentage of perennial fluvial facies starts to decrease, down to less than 3% recorded in the southernmost log (Cerro Padilla well, Figs. 8B, 10C).

The ephemeral fluvial facies association accounts for $\sim 30\%$ in the GA003 log (Figs. 8B, 10C). The proportion of the ephemeral fluvial facies association increases to the south radially along the system, showing an inverse relationship to the abundance of the perennial fluvial facies association (Figs. 8B, 10C). The two wells (Cañada del Charrua and Cerro Padilla) typify the distal increase in ephemeral fluvial facies and the decrease in perennial fluvial facies in the (SW) region (Figs. 8B, 10C).

The aeolian facies association is most abundant between 850 and 890 km downstream (17–19%), becoming a constant element but less abundant (7–26%) to the southwest (Figs. 8D, 10C). Floodplain facies become abundant around 980 km downstream, constituting between 25 and 30% of logs in the southern region of the study area (Fig. 8C, Fig. 10C).

Spearman's correlation of facies proportions versus downcurrent distance (Table 2) validates the above observations, indicating a strong downcurrent decrease in the occurrence of perennial facies and a characteristic increase in the abundance of ephemeral facies. Additionally, there is a statistically significant, moderately positive correlation in the abundance of floodplain and aeolian facies proportions with downcurrent distance (Table 2).

Channel-Body Thickness

Channel bodies with identifiable tops and bases were used to calculate the total channel-body thickness, and averages were calculated from this dataset. A general decrease in channel-body thickness is observed downsystem along a NE-to-SW transect, although the correlation is moderate and not demonstrably linear, as shown by the observed R_s coefficient and p value (Fig. 11A, Table 2). For the first 750 km, the channel bodies have an average thickness > 6 m. In the most distal third of the transect, however, the channel-body thickness decreases to < 5 m, and this low value is maintained to the most distal locations.

Number of Stories per Channel Body

The number of amalgamated stories per individual channel body decreases downstream from between 5 and 7 in the northeast to between 1 and 2 in the south (Fig. 11B). This trend has a weak negative correlation between the number of stories per channel-body distance ($R_s = -0.48$). A p value of 0.07 suggests that the correlation is not reliable. This weak correlation could be a result of a random distribution with small variations in the distal part of the system, where a significant part of the data was

collected. Despite this, the number of stories per preserved channel body clearly decreases downstream, from proximal to distal areas (Fig. 11B).

Average Story Thickness

The average story thickness in the Guará system varies from 0.75 m to 3.25 m, with an outlier of 7.65 at GA003 (Fig. 11C). The variation is distributed randomly along the NE–SW dip-oriented transect, as demonstrated also by an R_s coefficient of -0.0801 and a p value > 0.50 , indicating that there is no correlation between story thickness and distance downstream.

Average Bar Thickness

The average bar thickness was measured only in perennial fluvial facies associations because barforms were not recognized in ephemeral fluvial deposits of the Guará Formation. Estimated bar thickness varies from 0.6 m to 1.25 m, with an outlier of 1.64 m, showing no significant or abrupt changes in the size of preserved channel bars along the NE–SW dip-oriented transect (Fig. 11D). However, the observed R_s coefficient (-0.7091) demonstrates a strong negative statistical correlation between bar thickness and distance downstream, supported by a reliable p value of 0.02.

Weighted Average Grain Size of Fluvial Channel Bodies

This analysis considers the weighted average grain size of both perennial and ephemeral channel bodies. In the northern part (Paraná State) of the study area, coarse sand dominates (Figs. 11E, 12B). In western Rio Grande do Sul State, medium sand dominates (Figs. 11E, 12C). In the southernmost locations (Uruguay), fine sand dominates (Figs. 11E, 12C). The R_s coefficient (0.88, Fig. 11E) indicates a strong downstream-finishing trend, with strong correlation between distance downstream and observed grain size in fluvial channel-fill deposits. The low p value (0.001, Fig. 11E) further corroborates the strong correlation. The distribution suggests a proximal-to-distal zonation, with a downstream reduction in grain size from northeast to southwest in successions of the Guará System.

DISCUSSION

Depositional Model: the Guará Distributive Fluvial System

Guará DFS Multiparameter Zonation.—The facies analysis integrated with the spatial distribution of quantified properties of facies associations along a downstream transect across the basin suggests that the Guará Formation records deposition from a distributive fluvial system (DFS) interacting with aeolian dune fields in its distal sector, thus bearing attributes of a terminal fluvial megafan (Fig. 13). Similar interpretations were previously suggested by Amarante et al. (2019) and Reis et al. (2019).

Due to the spatial distribution of available outcrops across the studied region (i.e., allowing access to a downstream-oriented transect), the radial pattern of the paleocurrents, characteristic of ancient and modern distributive fluvial systems (Hartley et al. 2010; Weissmann et al. 2010, 2015), cannot be recognized in this study. On the other hand, the analysis of distribution of cross-bedding dip direction supports the quantification of the downstream trends, which is fundamental to recognizing spatial variations within successions of distributive fluvial systems (Owen et al. 2015). Both perennial and ephemeral fluvial facies associations show a general paleocurrent trend to the SSW (Fig. 7), suggesting that the proximal parts of the Guará distributive fluvial system were located in the Paraná State (Brazil) and that the most distal parts extended into present-day Uruguayan territory. It is possible that the system extended farther south, because the terminal limit of the Guará megafan cannot be determined based on available outcrop or well-core data. However, the increase in aeolian and floodplain deposits preserved in the distal part of

the succession (Figs. 8C, D, 10) suggests that the system likely did not extend much farther south than the limit of the study area.

The gradual transition of facies associations from proximal to distal parts suggests a longitudinal zonation of paleoenvironments and processes for the Guará system (Figs. 8, 10, 13), similar to that observed in modern distributive fluvial systems and DFS stratigraphic records (Kelly and Olsen 1993; Nichols and Fisher 2007; Cain and Mountney 2009; Weissmann et al. 2010, 2015; Davidson et al. 2013; Owen et al. 2015). The perennial fluvial facies association dominates the proximal part and decreases in abundance gradually downstream (Table 2), while ephemeral fluvial deposits appear in the interpreted medial to distal zone and increase in abundance toward the distal terminus of the system (Figs. 10, 8B, Table 2). This transition coincides with the appearance of aeolian deposits in the distal sector and with a downstream increase in preserved floodplain deposits.

Based on the quantitative spatial analyses, four zones are recognized in the Guará DFS and its preserved stratigraphy, from proximal to distal (Fig. 13):

Zone 1.—This is the most proximal part of the system, largely covered by active and inactive perennial channels. Frequent channel avulsions, controlled by sedimentation rates higher than accommodation, generate wide channel belts recorded as highly amalgamated multistory channel bodies, with very low preservation of floodplain deposits. The relatively reduced area in this proximal sector of the fan also enhances the potential for rapid reworking of the active fan surface by migrating channels, contributing to a coarse-grained-dominated stratigraphy. Channel-belt incision and coarse grain sizes are found in this zone.

Zone 2.—Perennial channel belts start to bifurcate, and although intense avulsion is still present, vast fan areas remain exposed for a longer time. Intense and episodic flood events promote widespread expansion and unconfinement of channel belts, recording ephemeral fluvial deposits as the aggradation of tabular sand sheets comprising transcritical- to supercritical-flow facies associations. The recurrence of perennial and ephemeral fluvial facies associations does not allow floodplain preservation, except for heterolithic lenses under highly erosional surfaces. Coarse to medium sand is deposited in this area.

Zone 3.—High dispersion and bifurcation of the perennial channel belts are recorded stratigraphically by channel bodies with less amalgamated stories. Larger areas are exposed for more time as the system expands laterally, with some areas affected only occasionally by ephemeral fluvial channels. This allows aeolian reworking of sandy alluvium to form aeolian sand sheets and the migration and accumulation of aeolian dunes. The availability of sand for aeolian transport is interrupted by new floods and by the migration of fluvial channel belts. Medium- to fine-grained sand dominates this zone.

Zone 4.—The terminal zone of the DFS. Channel discharge is dispersed into terminal splays, and only the distal fringes of ephemeral floods reach this zone, accumulating fine-grained deposits comprising waning-flow facies successions; fluvial channel bodies consist of single or at a maximum two stories. Aeolian systems are active here too. Only fine and very fine sand are accumulated in this terminal part of the DFS.

The proposed zonation of the Guará DFS is supported by other quantified parameters. The average grain size and the average bar thickness of the fluvial channel fills decrease linearly downstream (Fig. 11E, D). These reductions can be attributed to loss of discharge due to channel bifurcations, infiltration, and evapotranspiration (Nichols and Fisher 2007; Weissmann et al. 2010, 2013, 2015), which cause a decrease in the depth

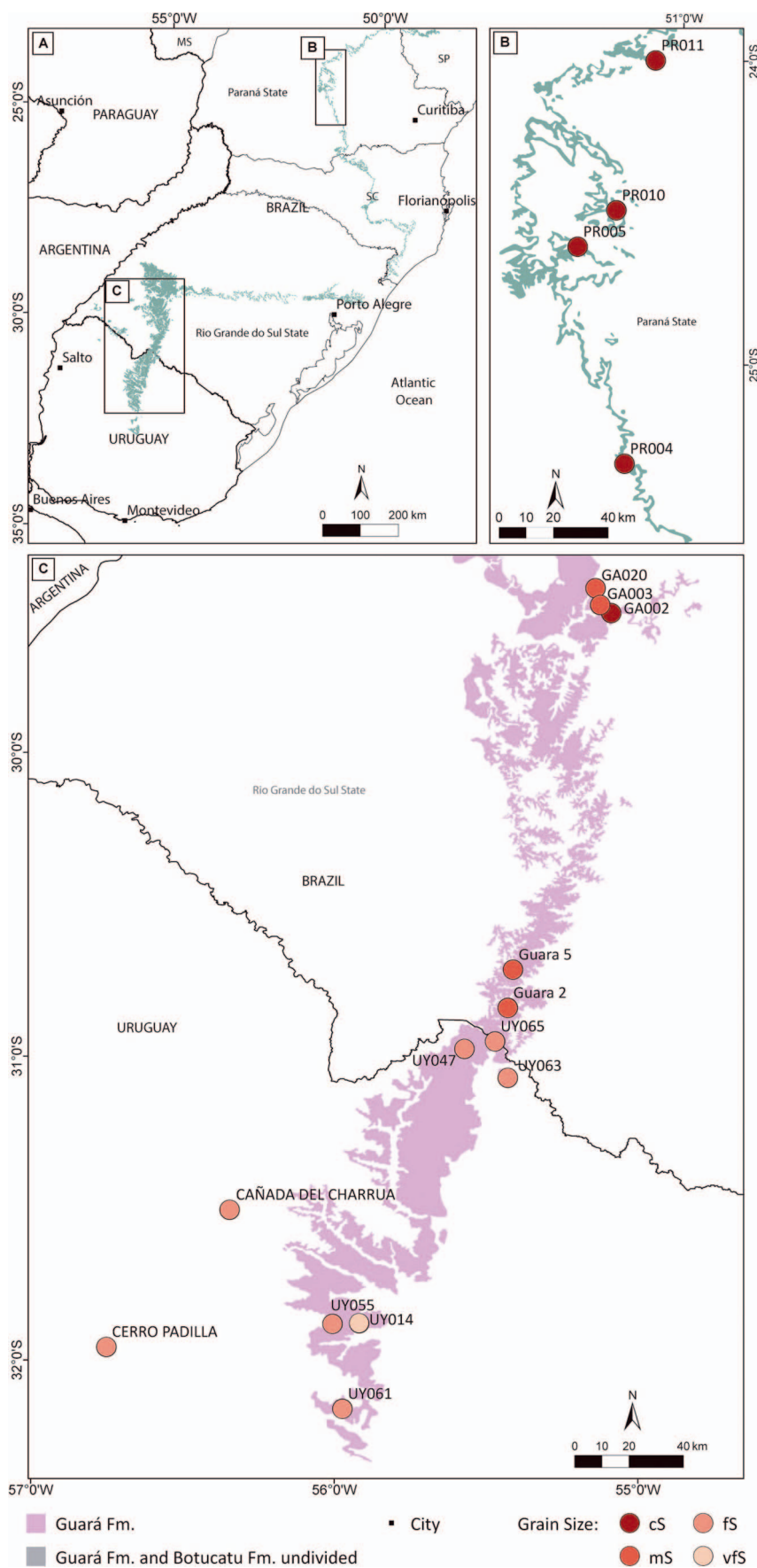


FIG. 12.—Map of the weighted average grain size of fluvial channels. A) Location of the study areas. B) Paraná State area. C) Rio Grande do Sul and Uruguay area.

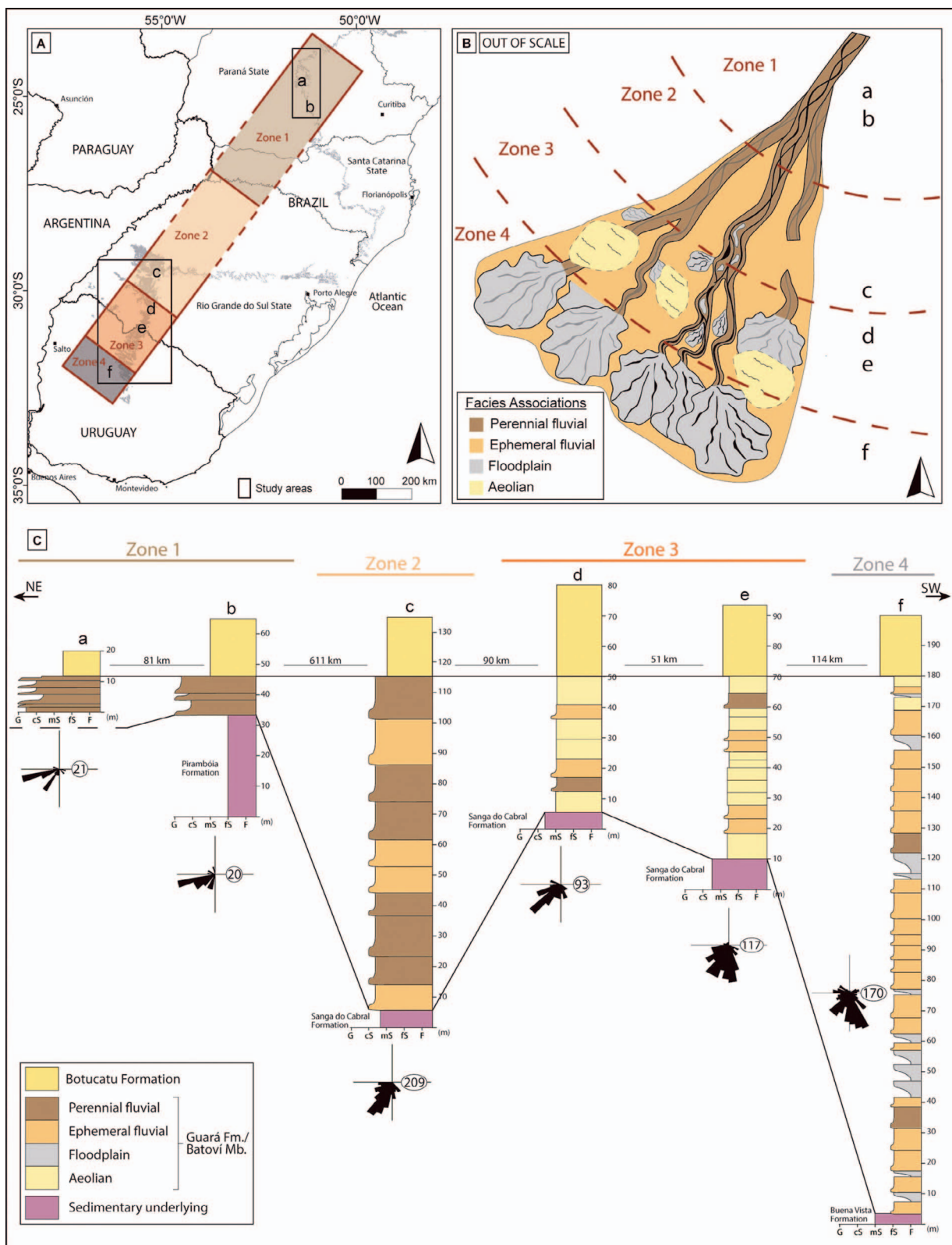


FIG. 13.—Depositional model of the Guará distributive fluvial system. **A)** Estimated area and distribution of the zonation in the Guará DFS area. **B)** Depositional model of the Guará DFS showing the spatial relations of facies associations in each zone. Not to scale. **C)** Composite logs representing the regional variations in Guará DFS. The relative distribution of facies associations and the grain size vary down-system. Location of the logs is in Figure 12A.

and competence of fluvial channels downstream. Downstream reduction in grain size is proposed by Weissmann et al. (2015) as one of the main criteria to recognize distributive fluvial systems in the rock record. A similar pattern was found in the Salt Wash DFS by Owen et al. (2015) as well as in the Huesca System by Hirst (1991). In comparison, tributary river systems tend not to maintain a regular grain-size reduction downstream, due to the input of different textural populations from tributary rivers; conversely, they may show an increase in grain size following the rise of discharge expected downstream (Davidson et al. 2013; Weissmann et al. 2015).

The downstream decreases in channel-body thickness identified in the Guará Formation (Fig. 11A, B) is consistent with DFS stratigraphic models. These features suggest reductions in channel-belt width due to bifurcation and loss of discharge from the proximal to distal part of the distributive system. Hartley et al. (2010) argue that a downstream reduction in discharge results in a reduction of channel depth and width as definitive characteristics of DFS. In dryland systems, the loss of discharge downstream by evapotranspiration and infiltration cannot be compensated due to the lack of tributary channels to feed the main channel belt. This argument has been contested by Fielding et al. (2012), invoking one of the most cited modern DFS, the Kosi Fan, to affirm that the discharge and size of the channel are not decreasing along the 120 km of that system. However, Weissmann et al. (2015), using modern LANDSAT orbital images of Kosi Fan, show that although the discharge and channel depth do not decrease downstream, the width and complexity of the Kosi River channel belts consistently decrease from the proximal to distal regions. In studies of the rock record such as this one, loss of discharge can be inferred only by indirect sedimentological evidence (such as reduced modal grain size of channel fills, reduction in the thickness of cross-strata (co)sets, and other parameters); thus downstream reduction in channel-body thickness and number of stories are considered here the best indirect indicators of downstream reduction in discharge for the Guará DFS model. However, the direct cause of loss in discharge (be it bifurcation, infiltration, evapotranspiration, or a combination thereof) could not be determined from the studied Guará DFS dataset.

Interestingly, story thickness shows no strong downstream trends (Fig. 11C). However, it is important to note that this may be due to lesser preservation potential for accumulating channel fills in the proximal region. It is well documented that avulsions occur over a small area in the proximal region compared to more distal realms of a DFS (Owen et al. 2015). It is, therefore, entirely possible that stories (elements representative of paleochannel depth) are not regularly preserved in the proximal sector, being more likely truncated by subsequent channel migration and superposition, whereas their preservation potential increases downstream. Martin et al. (2021) recognized that the story thickness can be highly variable in proximal to medial sectors of DFS successions and suggest caution when using this parameter to develop DFS models. The downstream reduction in channel-body thickness and in the number of stories alongside an increase in non-channel facies associations is related to a proximal-to-distal decrease in channel reworking and in the amalgamation of preserved channel fills (Weissmann et al. 2013; Owen et al. 2015; Burnham et al. 2020).

Terminal System and Aeolian Interaction: Comparison with Ancient and Modern DFSs

Paleocurrent pattern and associated facies characteristics from aeolian deposits indicate the presence of sinuous transversal chains of dunes with NW–SE orientation and migration in a NE direction (Fig. 7D, D1). When comparing fluvial and aeolian dune paleocurrent distributions (Fig. 7), in the majority of locations, these show opposing directions, suggesting no deflection and reorientation of the channels through the interdune space. This indicates no coalescence between aeolian dune fields and fluvial

channels, confirming the Scherer and Lavina (2005) interpretation of alternating fluvial and aeolian activity. An alternative interpretation is that if the river systems are large in comparison with dune size, then the river system could cross the dune field transversally to the dune-crest orientation. But, even in these systems, some deflection of the water flow is expected at the contact between river channels and dune fields (Al-Masrahy and Mountney 2015). For the Guará system, in southern locations, some paleocurrents of perennial fluvial and aeolian dune strata are perpendicular (Fig. 7B, D). However, the aeolian facies association is less abundant in this region in comparison with ephemeral fluvial and floodplain strata (Figs. 10, 8C, D), which points to no causal relationship for this specific paleocurrent distribution.

The facies zonation of the Guará DFS is similar to those described for terminal fluvial-fan successions recognized from the rock record (Kelly and Olsen 1993; Nichols and Fisher 2007; Cain and Mountney 2009). The tendency for a downstream reduction in channelization of the fluvial systems, for interaction with aeolian systems, and occurrence of terminal splays and waning-flow deposits in the distal parts are typical of terminal fans. Terminal fans in modern systems are typically established in endorheic basins in dry climates (Hartley et al. 2010).

The occurrence of aeolian deposits in distal zones of terminal fans was described by Kelly and Olsen (1993) as a common characteristic of terminal fans with low suspended load of muddy sediments, in which the aeolian deposits replace floodplain fines as interchannel deposits. Additionally, the origin of aeolian deposits is related to the ephemeral activity of dryland channel systems, which leaves vast areas of the fan exposed and only occasionally affected by floods, allowing significant aeolian reworking of exposed channel sediments (Kelly and Olsen 1993). Priddy and Clarke (2020) describe a similar setting where the ephemeral fluvial and aeolian activity are interrelated in a system with a lack of mud-grade sediments in the Lower Jurassic Kayenta Formation, USA. The authors attribute the lack of mud-grade sediments to the reworking of aeolian deposits by fluvial channels. The scarcity of muddy sediments is peculiar in the Guará Formation and could be attributed to fluvial reworking of aeolian deposits in distal zones. Even in the floodplain facies associations, mud-grade sediments account for less than 21% of the facies described (Fd, Fl, and Fm facies, excluding heterolithic associations (Ht); Fig 3). In the Guará DFS, aeolian deposits are concentrated in distal sectors 3 and 4 (Fig. 13), where the ephemeral fluvial facies association dominates over perennial fluvial.

Modern examples of DFSs with aeolian interaction are in the Tarim Basin (China). More than 80% of the area of the Tarim Basin is covered by aeolian dune fields, but analysis of LANDSAT images show traces of fluvial paleochannels overlapping dune fields (Weissmann et al. 2015), probably recording past expansion of the DFS into distal zones that currently host primarily aeolian activity and accumulation. Iriondo (1993) demonstrated how high-frequency climatic changes induce abrupt interaction among perennial and ephemeral fluvial channels and aeolian dune fields inside DFSs of the Chaco Plains, South America. Climatic changes were found to have influenced aeolian reworking of fluvial deposits in West Lake Eyre, Central Australia (Croke et al. 1998). Other examples of Quaternary fluvial–aeolian interactions in DFSs are reported in the Bolivian Chaco by Latrubesse et al. (2012) and in Lake Eyre Basin, Australia, by Cohen et al. (2010). Small DFSs in the Pampean Ranges, Argentina, show a zonation similar to facies-association distributions of the Guará DFS, where fluvial systems from proximal zones cross dune fields, ending in terminal splays in the most distal fringes (Santi Malnis et al. 2020). Davidson et al. (2013) presented a geomorphic model of DFSs in dryland climates in which extensive channel amalgamation is present in the proximal zone due to frequent nodal avulsion, while the distal part may be represented by a termination of the drainage system into an aeolian dune field and terminal-splay deposits as *braided bifurcating DFSs*. The study herein shows that the Guará DFS has several features in common with this

type of system. However, the braided character of fluvial channels is not clearly recognizable from the stratigraphy of the Guará DFS, because river planforms are not easily distinguished in the rock record, as pointed out by Fielding et al. (2018).

Accommodation Balance and Stratigraphic Complexity

The presence of a high-relief truncating surface up to 700 km down the system's radial extent (Fig. 6) is interpreted to be the result of fluvial incision over previous deposits. Incision and the occurrence of perennial fluvial channels in the most distal zones of the Guará System, normally reached only by ephemeral fluvial and terminal splays (Figs. 8, 10), may indicate a rearrangement in the drainage system's profile. This suggests an advance of the intersection point down-system, which defined a zone of low accommodation and dominant incision or bypass upstream and a zone of dominant aggradation downstream of the new intersection point (Weissmann et al. 2002). Incision in the proximal zones of the DFS could have been caused by climate-driven discharge fluctuations (Weissmann et al. 2002, 2005; Gibling et al. 2005; Fontana et al. 2008) or tectonic activity (Gawthorpe and Leeder 2000). Incision promoted by climatic cyclicity is common in modern DFSs, such as the Taquari River, Brazil (Assine 2005; Weissmann et al. 2015), and the western Ganges Plain, India (Gibling et al. 2005; Tandon et al. 2006; Kale 2007; Roy et al. 2012; Weissmann et al. 2015). Vertical trends in the Guará Formation are not observed herein, thus making it difficult to constrain a tectonic or climatic control. However, the alternation of perennial and ephemeral fluvial with aeolian deposits suggest high-frequency climatic variations. On the other hand, tectonic control cannot be discounted, although indirect sedimentologic evidence for that (e.g., abrupt vertical shifts in sediment caliber) is absent in the Guará Formation.

At outcrop scale, alternations of perennial and ephemeral channel bodies are identified in the proposed Zone 2 of the Guará DFS, as previously discussed by Reis (2016), who proposed a relation between these fluvial-style alternations and wetting-upward cycles interpreted by Scherer and Lavina (2005) in Zone 3. Both works suggest high-frequency orbital cycles as possible controls to those facies successions. Similar perennial and ephemeral interbedding is recognized in an Upper Cretaceous dryland DFS of the Bauru Group by Soares et al. (2018) and Martinelli et al. (2019). These authors also claim climate control of such fluvial-style alternation, reinforcing the value of fluvial successions as climate proxies in continental basins.

Nevertheless, the present study does not identify vertical trends (Fig. 9) that demonstrate progradation or retrogradation, or any clear cyclicity of Guará DFS deposits that are time correlatable across the system, as previously suggested by Scherer and Lavina (2005). It is possible that the basin scale of our study, plus the necessity of excluding some smaller outcrops from the dataset due to statistical representativity, excluded some of the best examples of wetting-drying cycles demonstrated by Scherer and Lavina (2005). Another possibility is that fluvial-aeolian cyclicity could be better recognized only in Zone 3 of the Guará DFS (the area of the Scherer and Lavina 2005 study), where aeolian deposits are more abundant.

Guará DFS Extent and Paleogeographic Implications

The Guará Formation records the largest DFS recognized from both modern and ancient datasets, as the minimum estimated extent of the Guará DFS is 1050 km (Fig. 13). This size exceeds the largest distributive fluvial system recorded in modern basins (the Pilcomayo DFS in the Bolivian Chaco basin, which has an apex-to-toe length of ~ 720 km; Hartley et al. 2010; Weissmann et al. 2010). The longest DFS estimated so far in the rock record is the Late Jurassic Salt Wash DFS in the western USA, with 550 km of extent (Owen et al. 2015). Latrubesse (2015)

estimated that the megafan system recorded in the Miocene Solimões Formation covered an area of 7,000,000 km², but the extent from proximal to distal is not known. The results presented here confirm how consistent DFS spatial trends can be over considerably greater spatial scales than commonly described.

Geodynamic Setting of the Guará Formation

The importance of the Upper Jurassic Guará Formation and Batoví Member in the Paraná Basin has been highlighted in several paleontological (Mones 1980; Martinez et al. 1993; Perea et al. 2001, 2003, 2014, 2018; Yanbin et al. 2004; Dentzien-Dias et al. 2008; Soto and Perea 2008, 2010; Fortier et al. 2011; Soto et al. 2012a, 2012b, 2020; Francischini et al. 2015, 2017; Mesa and Perea 2015) and sedimentological studies (Scherer and Lavina 2005, 2006; Soares et al. 2008; Perea et al. 2009; Reis 2016; Amarante et al. 2019; Reis et al. 2019) in Uruguayan and Brazilian territories. None of these works, however, explores the geodynamic significance of the Upper Jurassic units. Based on the quantified model presented here, we propose some points to open discussion about the tectono-sedimentary relevance of the Guará System to Western Gondwana.

Paleocurrent directions and recycled detrital composition suggest that the Guará Formation–Batoví Member system records a depocenter change in the Paraná Basin, with uplift of the central part and accommodation creation along the southwestern margin of the basin. The depositional model points to deposition in a wide intracratonic basin, likely related to the breakup of Gondwana (Reis et al. 2019).

The detrital source area for the Guará Formation is interpreted to have been located in the region northeast of the Paraná State outcrops (Brazil). The absence of the Guará Formation to the north of Paraná State (Fig. 13C) suggests that this region, covered by the ancient successions of the Paraná Basin, was subjected to erosion during the Late Jurassic. The homogeneity of the quartzarenite composition along the entire formation, the lack of a mud-grade fraction, and the occurrence of gravel lags of ancient sedimentary lithologies reinforce this recycling hypothesis.

The total thickness of the Guará Formation shows variations across the studied regions (Fig. 8A). The transect shows a general increase in formation thickness, which varies locally in the most distal zone. Scherer and Lavina (2006) suggested that the far-eastern part of the Guará Formation could have been controlled by a NW–SE-trending fault system. There is an abrupt interruption of the Guará Formation to the east beyond this fault system, where the overlying Botucatu Formation (Early Cretaceous) continues eastward. This suggests that the unconformity between the Late Jurassic Guará Formation and the Early Cretaceous Botucatu Formation would record faulting and erosion (Scherer and Lavina 2006; Amarante et al. 2019). Through seismic interpretation, Rossello et al. (2006, Fig. 7) identified thickness differences in Jurassic–Cretaceous sandstones that could be attributed to Mesozoic fault activity and erosion. Therefore, the deformation phase responsible for the thickness variability across the Guará Formation should have occurred after deposition and consolidation of the sedimentary unit.

Recent models that incorporate stratigraphic and thermochronologic data (Friedrich et al. 2018; Krob et al. 2020) relate tectonic subsidence and uplift in the entire Paraná Basin region to the Paraná–Etendeka plume activity, which started around 220 Ma and continued to the opening of the South Atlantic Ocean in the Early Cretaceous. These tectonic movements could have been responsible for accommodation creation during deposition of the Guará DFS, as well as for the successive faulting of its deposits. Unfortunately, the stratigraphic charts compiled by Krob et al. (2020) are based on interpretations from Milani et al. (2007), where the Guará Formation is not formally recognized as part of the depositional record of Late Jurassic sedimentation in the Paraná Basin. This warrants the urgent necessity for a revision of the stratigraphic framework of the Paraná Basin

to include this interval, as it is fundamental for new interpretations of the paleogeographic and tectonic evolution of western Gondwana.

CONCLUSIONS

- The Guará Formation and Batoví Member are here interpreted to record deposition by a large terminal megafan, with an estimated minimum length of 1,050 km, extending across present-day southern Brazil and Uruguay. The reconstructed geomorphic model for this system is similar to the braided bifurcating distributive fluvial system of Davidson et al. (2013).
- Four facies associations are recognized in the Guará Formation distributive fluvial system successions: perennial fluvial, ephemeral fluvial, floodplain, and aeolian deposits, indicating a dryland climatic regime.
- Quantitative analyses of sedimentologic parameters support the recognition of spatial trends following a NNE–SSW (downstream-oriented) direction. Spatial trends suggest a downstream reduction in channel depth, competence, and degree of channelization for the fluvial system, associated with increasingly reduced discharge downstream probably due to a combination of bifurcation, infiltration, and evapotranspiration.
- The large Guará DFS is divided into four zones, from proximal to distal sectors, defined from quantified spatial variations in sedimentary facies and architecture. Perennial fluvial channel-fills dominate zone 1; zone 2 comprises an alternation of ephemeral and perennial deposits, with the latter being dominant; in zone 3, perennial fluvial facies decrease while ephemeral fluvial facies increase in abundance and aeolian interchannel reworking is indicated; ephemeral fluvial deposits dominate in zone 4, with associated floodplain facies also present.
- The stratigraphic complexity of the Guará Formation suggests high-frequency fluctuations in discharge, causing recurrent expansion and retreat of the identified DFS zones, transferring the intersection point downstream, resulting in fluvial incision and erosion. Discharge fluctuations may have been related to cyclic climate variations affecting southwestern Gondwana in the Late Jurassic.
- The creation of accommodation for the deposition of the Guará Formation–Batoví Member and the later deformation and erosion of the unit, indicated by local variations in the preserved thickness of the successions, are attributed to the tectonic influence of the Paraná–Etendeka plume in the Paraná Basin region during the Upper Jurassic–Lower Cretaceous.

ACKNOWLEDGMENTS

This study was financed in part by the Coordenação de Aperfeiçoamento de Pessoal de Nível Superior–Brasil (CAPES)–Finance Code 001. A.D. Reis thanks the CNPq (Conselho Nacional de Desenvolvimento Científico e Tecnológico, process number 140453/2016-4) and the Programa de Recursos Humanos da Agência Nacional do Petróleo, Gás Natural e Biocombustíveis, PRH-ANP 14.1 (Resolução ANP nº 50/2015) for the scholarships provided along the project development. Bruno Angonese, Dina Cabrita, Monica Manna, Rossano Michel, and Thaís Schafer are acknowledged for help with pictures and review process, as well the colleagues of GEOSED Research Group UFRGS for field assistance. This work was significantly improved by the constructive comments from Brian Burnham, from the reviewers Dario Ventra and Giorgio Basilici, and from the JSR editors, to whom the authors are very grateful. The authors declare that they have no conflict of interests and the data that support the findings of this study are available from the corresponding author upon reasonable request.

REFERENCES

- ALIYUDA, K., HOWELL, J., USMAN, M.B., BELLO, A.M., MAINA, B., AND ABUBAKAR, U., 2019, Depositional variability of an ancient distributive fluvial system: the upper member of the lower cretaceous Bima Formation, Northern Benue Trough, Nigeria: *Journal of African Earth Sciences*, v. 159, p. 103600, doi: 10.1016/j.jafrearsci.2019.103600.
- ALLEN, J.P., FIELDING, C.R., GIBLING, M.R., AND RYGEL, M.C., 2014, Recognizing products of palaeoclimate fluctuation in the fluvial stratigraphic record: an example from the Pennsylvanian to Lower Permian of Cape Breton Island, Nova Scotia: *Sedimentology*, v. 61, p. 1332–1381, doi: 10.1111/sed.12102.
- ALLEN, J.R.L., 1963, The classification of cross-stratified units, with notes on their origin: *Sedimentology*, v. 2, p. 93–114, doi: 10.1111/j.1365-3091.1963.tb01204.x.
- ALLEN, J.R.L., AND LEEDER, M.R., 1980, Criteria for the instability of upper-stage plane beds: *Sedimentology*, v. 27, p. 209–217, doi: 10.1111/j.1365-3091.1980.tb01171.x.
- AL-MASRAHY, M.A., AND MOUNTNEY, N.P., 2015, A classification scheme for fluvial–aeolian system interaction in desert-margin settings: *Aeolian Research*, v. 17, p. 67–88, doi: 10.1016/J.AEOLIA.2015.01.010.
- AMARANTE, F.B. DO, SCHERER, C.M.S., GOSO AGUILAR, C.A., REIS, A.D. DOS MESA, V., AND SOTO, M., 2019, Fluvial–aeolian deposits of the Tacuarembó Formation (Norte Basin, Uruguay): depositional models and stratigraphic succession: *Journal of South American Earth Sciences*, v. 90, p. 355–376, doi: 10.1016/j.jsames.2018.12.024.
- ASSINE, M.L., 2005, River avulsions on the Taquari megafan, Pantanal wetland, Brazil: *Geomorphology*, v. 70, p. 357–371, doi: 10.1016/j.geomorph.2005.02.013.
- BRIDGE, J.S., AND BEST, J.L., 1988, Flow, sediment transport and bedform dynamics over the transition from dunes to upper-stage plane beds: implications for the formation of planar laminae: *Sedimentology*, v. 35, p. 753–763, doi: 10.1111/j.1365-3091.1988.tb01249.x.
- BRISTOW, C.S., 1987, Brahmaputra River: channel migration and deposition, in Ethridge, F.G., Flores, R.M., and Harvey, M.D., eds., *Recent Developments in Fluvial Sedimentology*: SEPM, Special Publication 39, p. 63–74.
- BROMLEY, M.H., 1991, Variations in fluvial style as revealed by architectural elements, Kayenta Formation, Mesa Creek, Colorado, USA: evidence for both ephemeral and perennial fluvial processes, in Miall, A.D., and Tyler, N., eds., *The Three-Dimensional Facies Architecture of Terrigenous Clastic Sediments and Its Implications for Hydrocarbon Discovery and Recovery*: SEPM, Concepts and in Sedimentology and Paleontology 3, p. 94–102.
- BURNHAM, B.S., AND HODGETTS, D., 2019, Quantifying spatial and architectural relationships from fluvial outcrops: *Geosphere*, v. 15, p. 236–253, doi: 10.1130/GES01574.1.
- BURNHAM, B.S., JERRETT, R.M., HODGETTS, D., AND FLINT, S.S., 2020, Discriminating stacked distributary channel from palaeovalley fill sand bodies in foreland basin settings: *Sedimentary Geology*, v. 398, p. 105592, doi: 10.1016/j.sedgeo.2020.105592.
- CAIN, S.A., AND MOUNTNEY, N.P., 2009, Spatial and temporal evolution of a terminal fluvial fan system: the Permian organ rock formation, south-east Utah, USA: *Sedimentology*, v. 56, p. 1774–1800, doi: 10.1111/j.1365-3091.2009.01057.x.
- CHRISTOFOLLETTI, B., PEIXOTO, B.C.P.M., WARREN, L. V., INGLEZ, L., FERNANDES, M.A., ALESSANDRETTI, L., ALEXANDRE DE JESUS PERINOTTO, J., SIMÓES, M.G., AND ASSINE, M.L., 2021, Dinos among the dunes: dinoturbation in the Pirambóia Formation (Paraná Basin), São Paulo State and comments on cross-section tracks: *Journal of South American Earth Sciences*, v. 109, p. 1–15, doi: 10.1016/j.jsames.2021.103252.
- CICCIOLI, P.L., MARENSSI, S.A., AMIDON, W.H., LIMARINO, C.O., AND KYLANDER-CLARK, A., 2018, Alluvial to lacustrine sedimentation in an endorheic basin during the Miocene: the Toro Negro Formation, Central Andes of Argentina: *Journal of South American Earth Sciences*, v. 84, p. 69–87, doi: 10.1016/j.jsames.2018.03.011.
- ÇİFTÇİ, N.B., AND BOZKURT, E., 2009, Evolution of the Miocene sedimentary fill of the Gediz Graben, SW Turkey: *Sedimentary Geology*, v. 216, p. 49–79, doi: 10.1016/j.sedgeo.2009.01.004.
- COHEN, T.J., NANSON, G.C., LARSEN, J.R., JONES, B.G., PRICE, D.M., COLEMAN, M., AND PIETSCH, T.J., 2010, Late Quaternary aeolian and fluvial interactions on the Cooper Creek Fan and the association between linear and source-bordering dunes, Strzelecki Desert, Australia: *Quaternary Science Reviews*, v. 29, p. 455–471, doi: 10.1016/J.QUASCIR.EV.2009.09.024.
- COLLINSON, J.D., 1996, Alluvial sediments, in Reading, H.G., ed., *Sedimentary Environments: Processes, Facies and Stratigraphy*, Third Edition: Blackwell Publishing, p. 37–82.
- COLLINSON, J.D., MOUNTNEY, N., AND THOMPSON, D., 2006, *Sedimentary Structures*: Hertfordshire, Terra Publications, 292 p.
- CROKE, J.C., MAGEE, J.M., AND PRICE, D.M., 1998, Stratigraphy and sedimentology of the lower Neales River, West Lake Eyre, Central Australia: from Palaeocene to Holocene: Palaeogeography, Palaeoclimatology, Palaeoecology, v. 144, p. 331–350, doi: 10.1016/S0031-0182(98)00125-4.
- DAI' BÓ, P.F., SOARES, M.V.T., BASILICI, G., RODRIGUES, A.G., AND MENEZES, M.N., 2019, Spatial variations in distributive fluvial system architecture of the Upper Cretaceous Marília Formation, SE Brazil: *Geological Society of London, Special Publication* 488, p. 97–118, doi: 10.1144/SP488.6.
- DAVIDSON, S.K., HARTLEY, A.J., WEISSMANN, G.S., NICHOLS, G.J., AND SCUDERI, L.A., 2013, Geomorphic elements on modern distributive fluvial systems: *Geomorphology*, v. 180–181, p. 82–95, doi: 10.1016/j.geomorph.2012.09.008.
- DAVIS, J.C., 2002, *Statistics and Data Analysis in Geology*, Third Edition: John Wiley and Sons, 638 p.
- DECELLES, P.G., AND CAVAZZA, W., 1999, A comparison of fluvial megafans in the Cordilleran (Upper Cretaceous) and modern Himalayan foreland basin systems: *Geological Society of America, Bulletin*, v. 111, p. 1315–1334, doi: 10.1130/0016-7606(1999)111<1315:ACOFMI>2.3.CO;2.

- DENTZEN-DIAS, P.C., SCHULTZ, C.L., AND BERTONI-MACHADO, C., 2008, Taphonomy and paleoecology inferences of vertebrate ichnofossils from Guar?? Formation (Upper Jurassic), southern Brazil: *Journal of South American Earth Sciences*, v. 25, p. 196–202, doi:10.1016/j.jsames.2007.08.008.
- DONSELAAR, M.E., CUEVAS GOZOLO, M.C., AND MOYANO, S., 2013, Avulsion processes at the terminus of low-gradient semi-arid fluvial systems: lessons from the Río Colorado, Altiplano endorheic basin, Bolivia: *Sedimentary Geology*, v. 283, p. 1–14, doi:10.1016/j.sedgeo.2012.10.007.
- FIELDING, C.R., ALLEN, J.P., ALEXANDER, J., GIBLING, M.R., RYGEL, M.C., AND CALDER, J.H., 2011, Fluvial systems and their deposits in hot, seasonal semiarid and subhumid settings: modern and ancient examples, in Davidson, S.K., Leleu, S., and North, C.P., eds., *From River to Rock Record: The Preservation of Fluvial Sediments and Their Subsequent Interpretation*: SEPM, Special Publication 97, p. 89–111, doi:10.2110/sepmsp.097.089.
- FIELDING, C.R., ASHWORTH, P.J., BEST, J.L., PROKOCKI, E.W., AND SMITH, G.H.S., 2012, Tributary, distributary and other fluvial patterns: What really represents the norm in the continental rock record?: *Sedimentary Geology*, v. 261–262, p. 15–32, doi:10.1016/j.sedgeo.2012.03.004.
- FIELDING, C.R., ALEXANDER, J., AND ALLEN, J.P., 2018, The role of discharge variability in the formation and preservation of alluvial sediment bodies: *Sedimentary Geology*, v. 365, p. 1–20, doi:10.1016/j.sedgeo.2017.12.022.
- FONTANA, A., MOZZI, P., AND BONDÉSAN, A., 2008, Alluvial megafans in the Venetian–Friulian Plain (north-eastern Italy): evidence of sedimentary and erosive phases during Late Pleistocene and Holocene: *Quaternary International*, v. 189, p. 71–90, doi:10.1016/j.quaint.2007.08.044.
- FORTIER, D., PEREA, D., AND SCHULTZ, C., 2011, Redescription and phylogenetic relationships of *Meridiosaurus vallisparadisi*, a pholidosaurid from the Late Jurassic of Uruguay: *Zoological Journal of the Linnean Society*, v. 163, p. S257–S272, doi:10.1111/j.1096-3642.2011.00722.x.
- FRANCISCHINI, H., DENTZEN-DIAS, P.C., FERNANDES, M.A., AND SCHULTZ, C.L., 2015, Dinosaur ichnofauna of the Upper Jurassic–Lower Cretaceous of the Paraná Basin (Brazil and Uruguay): *Journal of South American Earth Sciences*, v. 63, p. 180–190, doi:10.1016/j.jsames.2015.07.016.
- FRANCISCHINI, H., SALES, M.A.F., DENTZEN-DIAS, P.C., AND SCHULTZ, C.L., 2017, The presence of Ankylosaur tracks in the Guará Formation (Brazil) and remarks on the spatial and temporal distribution of Late Jurassic Dinosaurs: *Ichnos*, v. 25, p. 177–191, doi:10.1080/10420940.2017.1337573.
- FRIEDRICH, A.M., BUNGE, H.P., RIEGER, S.M., COLLI, L., GHELICHKHAN, S., AND NERLICH, R., 2018, Stratigraphic framework for the plume mode of mantle convection and the analysis of interregional unconformities on geological maps: *Gondwana Research*, v. 53, p. 159–188, doi:10.1016/j.gr.2017.06.003.
- FRYBERGER, S.G., AHLBRANDT, T.S., AND ANDREWS, S., 1979, Origin, sedimentary features, and significance of low-angle eolian “sand sheet” deposits, Great Sand Dunes National Monument and vicinity, Colorado: *Journal of Sedimentary Petrology*, v. 49, p. 733–746, doi:10.1306/212F782E-2B24-11D7-8648000102C1865D.
- GALLOWAY, W.E., WHITEAKER, T.L., AND GANEY-CURRY, P., 2011, History of Cenozoic North American drainage basin evolution, sediment yield, and accumulation in the Gulf of Mexico basin: *Geosphere*, v. 7, p. 938–973, doi:10.1130/ges00647.1.
- GAWTHORPE, R.L., AND LEEDER, M.R., 2000, Tectono-sedimentary evolution of active extensional basins: *Basin Research*, v. 12, p. 195–218, doi:10.1111/j.1365-2117.2000.00121.x.
- GIBLING, M.R., TANDON, S.K., SINHA, R., AND JAIN, M., 2005, Discontinuity-bounded alluvial sequences of the southern Gangetic Plains, India: aggradation and degradation in response to monsoonal strength: *Journal of Sedimentary Research*, v. 75, p. 369–385, doi:10.2110/jsr.2005.029.
- HAMPTON, B.A., AND HORTON, B.K., 2007, Sheetflow fluvial processes in a rapidly subsiding basin, Altiplano plateau, Bolivia: *Sedimentology*, v. 54, p. 1121–1147, doi:10.1111/j.1365-3091.2007.00875.x.
- HARMS, J.C., SOUTHDARD, J.B., SPEARING, D.R., AND WALKER, R.G., 1982, Structures and Sequences in Clastic Rocks: SEPM, Short Course Notes 9, p. 161 p.
- HARTLEY, A.J., WEISSMANN, G.S., NICHOLS, G.J., AND WARWICK, G.L., 2010, Large distributive fluvial systems: characteristics, distribution, and controls on development: *Journal of Sedimentary Research*, v. 80, p. 167–183, doi:10.2110/jsr.2010.016.
- HEIN, F.J., AND WALKER, R.G., 1977, Bar evolution and development of stratification in the gravelly, braided Kicking Horse River, British Columbia: *Canadian Journal of Earth Sciences*, v. 14, p. 562–570.
- HERBERT, C.M., ALEXANDER, J., AMOS, K.J., AND FIELDING, C.R., 2019, Unit bar architecture in a highly-variable fluvial discharge regime: examples from the Burdekin River, Australia: *Sedimentology*, v. 67, p. 576–605, doi:10.1111/sed.12655.
- HIRST, J.P.P., 1991, Variations in alluvial architecture across the Oligo-Miocene Huesca Fluvial System, Ebro Basin, Spain, in Miall, A.D., and Tyler, N., eds., *The Three-Dimensional Facies Architecture of Terrigenous Clastic Sediments and Its Implications for Hydrocarbon Discovery and Recovery*: SEPM, Concepts in Sedimentology and Paleontology, v. 3, p. 111–121, doi:10.2110/csp.91.03.0111.
- HUNTER, R.E., 1977, Terminology of cross-stratified sedimentary layers and climbing-ripple structures: *Journal of Sedimentary Research*, v. 47, p. 697–706.
- HUNTER, R.E., AND RUBIN, D.M., 1983, Interpreting cyclic crossbedding, with an example from the Navajo Sandstone, in Brookfield, M.E. and Ahlbrandt, T.S., eds., *Eolian Sediments and Processes*: Elsevier, p. 429–454.
- IRIONDO, M., 1993, Geomorphology and late Quaternary of the Chaco (South America): *Geomorphology*, v. 7, p. 289–303, doi:10.1016/0169-555X(93)90059-B.
- JAMES, N.P., AND DALRYMPLE, R.W., 2010, Facies Models 4: The Geological Association of Canada, 586 p.
- JO, H.R., AND CHOUGH, S.K., 2001, Architectural analysis of fluvial sequences in the Northwestern part of Kyongsang Basin (Early Cretaceous), SE Korea: *Sedimentary Geology*, v. 144, p. 307–334, doi:10.1016/S0037-0738(01)00123-3.
- JONES, F.H., SCHERER, C.M. DOS S. AND KUCHLE, J., 2016, Facies architecture and stratigraphic evolution of aeolian dune and interdune deposits, Permian Caldeirão Member (Santa Brígida Formation), Brazil: *Sedimentary Geology*, v. 337, p. 133–150, doi:10.1016/j.sedgeo.2016.03.018.
- KALE, V.S., 2007, Fluvio-sedimentary response of the monsoon-fed Indian rivers to Late Pleistocene–Holocene changes in monsoon strength: reconstruction based on existing ^{14}C dates: *Quaternary Science Reviews*, v. 26, p. 1610–1620, doi:10.1016/j.quascirev.2007.03.012.
- KELLY, S.B., AND OLSEN, H., 1993, Terminal fans: a review with reference to Devonian examples: *Sedimentary Geology*, v. 85, p. 339–374, doi:10.1016/0037-0738(93)90092-J.
- KOCUREK, G., 1981, Significance of interdune deposits and bounding surfaces in aeolian dune sands: *Sedimentology*, v. 28, p. 753–780, doi:10.1111/j.1365-3091.1981.tb01941.x.
- KOCUREK, G., AND FIELDER, G., 1982, Adhesion structures: *Journal of Sedimentary Petrology*, v. 52, p. 1229–1241, doi:10.1306/2128102-2b24-11d7-8648000102C1865d.
- KROB, F.C., GLASMACHER, U.A., BUNGE, H.-P., FRIEDRICH, A.M., AND HACKSPACHER, P.C., 2020, Application of stratigraphic frameworks and thermostratigraphic data on the Mesozoic SW Gondwana intraplate environment to retrieve the Paraná–Etendeka plume movement: *Gondwana Research*, v. 84, p. 81–110, doi:10.1016/j.gr.2020.02.010.
- LATRUBESSE, E.M., 2015, Large rivers, megafans and other Quaternary avulsive fluvial systems: a potential “who’s who” in the geological record: *Earth-Science Reviews*, v. 146, p. 1–30, doi:10.1016/j.earscirev.2015.03.004.
- LATRUBESSE, E.M., STEVAUX, J.C., CREMON, E.H., MAY, J.H., TATUMI, S.H., HURTADO, M.A., BEZADA, M., AND ARGOLLO, J.B., 2012, Late Quaternary megafans, fans and fluvio-aeolian interactions in the Bolivian Chaco, tropical South America: *Palaeogeography, Palaeoclimatology, Palaeoecology*, v. 356–357, p. 75–88, doi:10.1016/j.PALAEO.2012.04.003.
- LINOL, B., DE WIT, M.J., MILANI, E.J., GUILLOCHEAU, F., AND SCHERER, C., 2015, New regional correlations between the Congo, Paraná and Cape–Karoo basins of southwest Gondwana, in de Wit, M., and Guillocheau, F., eds., *Geology and Resource Potential of the Congo Basin, Regional Geology Reviews*: Berlin, Springer, p. 245–268, doi:10.1007/978-3-642-29482-2_13.
- MARTIN, B., OWEN, A., NICHOLS, G.J., HARTLEY, A.J., AND WILLIAMS, R.D., 2021, Quantifying downstream, vertical and lateral variation in fluvial deposits: implications from the Huesca distributive fluvial system: *Frontiers in Earth Science*, v. 8, p. 564017 doi:10.3389/feart.2020.564017.
- MARTINELLI, A.G., BASILICI, G., FIORELLI, L.E., KLOCK, C., KARFUNKEL, J., DINIZ, A.C., SOARES, M.V.T., MARCONATO, A., DA SILVA, J.I., RIBEIRO, L.C.B., AND MARINHO, T.S., 2019, Palaeoecological implications of an Upper Cretaceous tetrapod burrow (Bauru Basin; Peirópolis, Minas Gerais, Brazil): *Palaeogeography, Palaeoclimatology, Palaeoecology*, v. 528, p. 147–159, doi:10.1016/j.PALAEO.2019.05.015.
- MARTINEZ, S., FIGUEIRAS, A., AND DA SILVA, J.S., 1993, A new Unionoidea (Mollusca, Bivalvia) from the Tacuarembó Formation (Upper Triassic–Upper Jurassic), Uruguay: *Journal of Paleontology*, v. 67, p. 962–965.
- MESA, V., AND PEREA, D., 2015, First record of Theropod and Ornithopod tracks and detailed description of Sauropod trackways from the Tacuarembó Formation (Late Jurassic–Early Cretaceous) of Uruguay: *Ichnos*, v. 22, p. 109–121, doi:10.1080/10420940.2015.1030075.
- MIALL, A.D., 1977, A review of the braided-river depositional environment: *Earth-Science Reviews*, v. 13, p. 1–62.
- MIALL, A.D., 1978, Lithofacies types and vertical profile models in braided river deposits: a summary, in Miall, A.D., ed., *Fluvial Sedimentology*: Canadian Society of Petroleum Geologists, Special Publication 5, p. 587–604.
- MIALL, A.D., 1985, Architectural-element analysis: a new method of facies analysis applied to fluvial deposits: *Earth-Science Reviews*, v. 22, p. 261–308, doi:10.1016/0012-8252(85)90001-7.
- MIALL, A.D., 1988, Reservoir heterogeneities in fluvial sandstones: lessons from outcrop studies: *American Association of Petroleum Geologists, Bulletin*, v. 72, p. 682–697.
- MIALL, A.D., 1996, *The Geology of Fluvial Deposits*: Berlin, Springer, 582 p.
- MILANI, E.J., 1997, Evolução tectono-estratigráfica da Bacia do Paraná e seu relacionamento com a geodinâmica fanerozoíca do Gondwana Sul-Oidental [Ph.D. Thesis]: Universidade Federal do Rio Grande do Sul, 255 p.
- MILANI, E.J., FACCINI, U.F., SCHERER, C.M., ARAÚJO, L.M., AND CUPERTINO, J.A., 1998, Sequences and stratigraphic hierarchy of the Paraná Basin (Ordovician to Cretaceous), Southern Brazil: *Boletim Instituto de Geociências Universidade de São Paulo, Série Científica*, v. 29, p. 125–173.
- MILANI, E.J., HENRIQUE, J., MELO G. DE, SOUZA, P.A. DE, FERNANDES, L.A., AND FRANÇA, A.B., 2007a, Bacia do Paraná: *Boletim de Geociências da Petrobras*, v. 15, p. 265–287.
- MILANI, E.J., HENRIQUE, J., MELO G. DE, SOUZA, P.A. DE, FERNANDES, L.A., AND FRANÇA, A.B., 2007b, Bacia do Paraná: *Boletim de Geociências da Petrobras*, v. 15, p. 265–287.
- MONES, A., 1980, Nuevos elementos de la paleoherpetofauna del Uruguay (Crocodilia e Dinosauria): *Congreso Latinoamericano de Paleontología, Resumenes*, p. 265–277.

- MOROZOVA, G.S., AND SMITH, N.D., 1999, Holocene avulsion history of the lower Saskatchewan fluvial system, Cumberland Marshes, Saskatchewan-Manitoba, Canada, in Smith, N.D., and Rogers, J., eds., Fluvial Sedimentology VI: International Association of Sedimentologists, Special Publication 28, p. 231–249.
- MOUNTNEY, N.P., AND THOMPSON, D.B., 2002, Stratigraphic evolution and preservation of aeolian dune and damp/wet interdune strata: an example from the Triassic Helsby Sandstone Formation, Cheshire Basin, UK: *Sedimentology*, v. 49, p. 805–833, doi:10.1046/j.1365-3091.2002.00472.x.
- MOUNTNEY, N., HOWELL, J., FLINT, S., AND JERRAM, D., 1998, Aeolian and alluvial deposition within the Mesozoic Etjo Sandstone Formation, northwest Namibia: *Journal of African Earth Sciences*, v. 27, p. 175–192, doi:10.1016/S0899-5362(98)00056-6.
- NICHOLS, G.J., AND FISHER, J.A., 2007, Processes, facies and architecture of fluvial distributary system deposits: *Sedimentary Geology*, v. 195, p. 75–90, doi:10.1016/j.sedgeo.2006.07.004.
- NICHOLS, G.J., AND HIRST, J.P., 1998, Alluvial fans and fluvial distributary systems, Oligo-Miocene, northern Spain: contrasting processes and products: *Journal of Sedimentary Research*, v. 68, p. 879–889, doi:10.2110/jsr.68.879.
- OWEN, A., EBINGHAUS, A., HARTLEY, A.J., SANTOS, M.G.M., AND WEISSMANN, G.S., 2017, Multi-scale classification of fluvial architecture: an example from the Palaeocene-Eocene Bighorn Basin, Wyoming: *Sedimentology*, v. 64, p. 1572–1596, doi:10.1111/sed.12364.
- RETLACK, G.J., 1988, Paleosols and weathering through geologic time: principles and applications: Geological Society of America, Special Paper 216, p. 1–20.
- ROSSELLO, E.A., VEROVSKY, G., SANTA ANA, H. DE FÚLFARO, V.J., AND FERNÁNDEZ GARRASINO, C.A., 2006, La Dorsal Asunción-Río Grande: un altofondo regional entre las cuencas Paraná (Brasil, Paraguay y Uruguay) y Chacoparanaense (Argentina): *Revista Brasileira de Geociências*, v. 36, p. 535–549.
- ROSSETTI, L., LIMA, E.F., WAIHEL, B.L., HOLE, M.J., SIMÕES, M.S., AND SCHERER, C.M.S., 2017, Lithostratigraphy and volcanology of the Serra Geral Group, Paraná-Itendeka Igneous Province in Southern Brazil: towards a formal stratigraphical framework: *Journal of Volcanology and Geothermal Research*, v. 355, p. 1–17, doi:10.1016/j.jvolgeores.2017.05.008.
- ROY, N.G., SINHA, R., AND GIBLING, M.R., 2012, Aggradation, incision and interfluvial flooding in the Ganga Valley over the past 100,000 years: testing the influence of monsoonal precipitation: *Palaeogeography, Palaeoclimatology, Palaeoecology*, v. 356–357, p. 38–53, doi:10.1016/j.palaeo.2011.08.012.
- SANTI MALNIS, P., ROTHIS, L.M., AND COLOMBI, C.E., 2020, Distributary drainage systems in La Huerta Range, western Pampean Ranges, San Juan, Argentina, p. 136–157, doi:10.1007/978-3-030-22621-3_7.
- SCHERER, C.M.S., AND GOLDBERG, K., 2007, Palaeowind patterns during the latest Jurassic-earliest Cretaceous in Gondwana: evidence from aeolian cross-strata of the Botucatu Formation, Brazil: *Palaeogeography, Palaeoclimatology, Palaeoecology*, v. 250, p. 89–100, doi:10.1016/j.palaeo.2007.02.018.
- SCHERER, C.M.S., AND LAVINA, E.L.C., 2005, Sedimentary cycles and facies architecture of aeolian-fluvial strata of the Upper Jurassic Guará Formation, southern Brazil: *Sedimentology*, v. 52, p. 1323–1341, doi:10.1111/j.1365-3091.2005.00746.x.
- SCHERER, C.M.S., AND LAVINA, E.L.C., 2006, Stratigraphic evolution of a fluvial-aeolian succession: the example of the Upper Jurassic-Lower Cretaceous Guará and Botucatu formations, Paraná Basin, southernmost Brazil: *Gondwana Research*, v. 9, p. 475–484, doi:10.1016/j.gr.2005.12.002.
- SCHERER, C.M.S., FACCINI, U.F., AND LAVINA, E.L., 2000, Arcabouço estratigráfico do Mesozóico da Bacia do Paraná, in Holz, M., and De Ros, L.F., eds., *Geologia Do Rio Grande Do Sul: Porto Alegre*, Editora da Universidade, p. 335–354.
- SCHERER, C.M.S., LAVINA, E.L.C., DIAS FILHO, D.C., OLIVEIRA, F.M., BONGIOLI, D.E., AND AGUIAR, E.S., 2007, Stratigraphy and facies architecture of the fluvial-aeolian-lacustrine Sergi Formation (Upper Jurassic), Recôncavo Basin, Brazil: *Sedimentary Geology*, v. 194, p. 169–193, doi:10.1016/j.sedgeo.2006.06.002.
- SCHERER, C.M.S., GOLDBERG, K., AND BARDOLO, T., 2015, Facies architecture and sequence stratigraphy of an early post-rift fluvial succession, Aptian Barbalha Formation, Araripe Basin, northeastern Brazil: *Sedimentary Geology*, v. 322, p. 43–62, doi:10.1016/j.sedg eo.2015.03.010.
- OWEN, A., NICHOLS, G.J., HARTLEY, A.J., WEISSMANN, G.S., AND SCUDERI, L.A., 2015, Quantification of a distributive fluvial system: the Salt Wash DFS of the Morrison Formation, SW U.S.A.: *Journal of Sedimentary Research*, v. 85, p. 544–561, doi:10.2110/jsr.2015.35.
- OWEN, A., HARTLEY, A.J., EBINGHAUS, A., WEISSMANN, G.S., AND SANTOS, M.G.M., 2019, Basin-scale predictive models of alluvial architecture: constraints from the Palaeocene-Eocene, Bighorn Basin, Wyoming, USA: *Sedimentology*, v. 66, p. 736–763, doi:10.1111/sed.12515.
- OWEN, G., AND MORETTI, M., 2011, Identifying triggers for liquefaction-induced soft-sediment deformation in sands: *Sedimentary Geology*, v. 235, p. 141–147, doi:10.1016/j.sedgeo.2010.10.003.
- PEREA, D., UBILLA, M., ROJAS, A., AND GOSO, C., 2001, The West Gondwanan occurrence of the hybodontid shark *Priohyodus*, and the late Jurassic-Early Cretaceous age of the Tacuarembó Formation, Uruguay: *Palaeontology*, v. 44, p. 1227–1235, doi:10.1111/1475-4983.00222.
- PEREA, D., UBILLA, M., AND ROJAS, A., 2003, First report of theropods from the Tacuarembó Formation (Late Jurassic-Early Cretaceous), Uruguay: *Alcheringa*, v. 27, p. 79–83, doi:10.1080/03115510308619548.
- PEREA, D., SOTO, M., VEROVSKY, G., MARTÍNEZ, S., AND UBILLA, M., 2009, A Late Jurassic fossil assemblage in Gondwana: biostratigraphy and correlations of the Tacuarembó Formation, Paraná Basin, Uruguay: *Journal of South American Earth Sciences*, v. 28, p. 168–179, doi:10.1016/j.jsames.2009.03.009.
- PEREA, D., SOTO, M., STERLI, J., MESA, V., TORIÑO, P., ROLAND, G., AND DA SILVA, J., 2014, *Tacuarembemys kusterae*, gen. et sp. nov., a new Late Jurassic-?Earliest Cretaceous continental turtle from western Gondwana: *Journal of Vertebrate Paleontology*, v. 34, p. 1329–1341, doi:10.1080/02724634.2014.859620.
- PEREA, D., SOTO, M., TORIÑO, P., MESA, V., AND MAISEY, J.G., 2018, A Late Jurassic-? Earliest Cretaceous stenochasmatid (Pterosauria, Pterodactyloidea): the first report of pterosaurs from Uruguay: *Journal of South American Earth Sciences*, v. 85, p. 298–306, doi:10.1016/j.jsames.2018.05.011.
- PRIDDY, C., AND CLARKE, S.M., 2020, The sedimentology of an ephemeral fluvial-aeolian succession: *Sedimentology*, v. 61, p. 2392–2425, doi:10.1111/sed.12706.
- PRIMM, J.W., JOHNSON, C.L., AND STEARNS, M., 2018, Basin-axial progradation of a sediment supply driven distributive fluvial system in the Late Cretaceous southern Utah foreland: *Basin Research*, v. 30, p. 249–278, doi:10.1111/bre.12252.
- REIS, A.D., DOS, 2016, Análise arquitetural de depósitos fluviais da Formação Guará (Jurássico Superior-Cretáceo Inferior) na borda sudeste da Bacia do Paraná, RS, Brasil [M.Sc. Thesis]: Universidade Federal do Rio Grande do Sul, 39 p.
- REIS, A.D., DOS, SCHERER, C.M. DOS S., AMARANTE, F.B. DO, ROSSETTI, M. DE M.M., KIFUMBI, C., SOUZA, E.G. DE FERRONATO, J.P.F., AND OWEN, A., 2019, Sedimentology of the proximal portion of a large-scale, Upper Jurassic fluvial-aeolian system in Paraná Basin, southwestern Gondwana: *Journal of South American Earth Sciences*, v. 95, p. 102248, doi:10.1016/j.jsames.2019.102248.
- SCHERER, C.M. DOS S., LAVINA, E.L.C., REIS, A.D., DOS AND HORN, B.L.D., 2021, Estratigrafia da sucessão sedimentar mesozóica da Bacia do Paraná no Rio Grande do Sul, in Jelinek, A.R., and Sommer, C.A., eds., *Contribuições à Geologia do Rio Grande do Sul e de Santa Catarina: Sociedade Brasileira de Geologia Núcleo RS/SC, Compasso Lugar-Cultura*, p. 289–304.
- SCHMITT, R.S., AND ROMEIRO, M.A.T., 2017, Gondwana Geological Map: Gondwana Project, http://www.gondwana.geologia.ufrr.br/br/?page_id=26.
- SOARES, P.C., 1975, Divisão estratigráfica do Mesozóico no estado de São Paulo: *Revista Brasileira de Geociências*, v. 5, p. 229–251.
- SOARES, A.P., SOARES, P.C., AND HOLZ, M., 2008, Correlações estratigráficas conflitantes no limite Permo-Triássico no Sul da bacia do Paraná: o contato entre duas seqüências e implicações na configuração espacial do aquífero Guarani: *Revista Pesquisa em Geociências*, v. 35, p. 115–133.
- SOARES, M.V.T., BASILICI, G., DAL' BÓ, P.F., DA SILVA MARINHO, T., MOUNTNEY, N.P., COLOMBERA, L., DE OLIVEIRA, E.F., AND DA SILVA, K.E.B., 2018, Climatic and geomorphologic cycles in a semiarid distributive fluvial system, Upper Cretaceous, Bauru Group, SE Brazil: *Sedimentary Geology*, v. 372, p. 75–95, doi:10.1016/j.sedg eo.2018.05.001.
- SOTO, M., AND PEREA, D., 2008, A Ceratosaurid (Dinosauria, Theropoda) from the Late Jurassic-Early Cretaceous of Uruguay: *Journal of Vertebrate Paleontology*, v. 28, p. 439–444.
- SOTO, M., AND PEREA, D., 2010, Late Jurassic lungfishes (Dipnoi) from Uruguay, with comments on the systematics of Gondwanan ceratodontiforms: *Journal of Vertebrate Paleontology*, v. 30, p. 1049–1058, doi:10.1080/02724634.2010.483540.
- SOTO, M., CARVALHO, M.S.S., MAISEY, J.G., PEREA, D., AND SILVA, J., 2012a, Coelacanth remains from the Late Jurassic-?earliest Cretaceous of Uruguay: the southernmost occurrence of the Mawsoniidae: *Journal of Vertebrate Paleontology*, v. 32, p. 530–537, doi:10.1080/02724634.2012.660899.
- SOTO, M., PEREA, D., AND TORINO, P., 2012b, New remains of *Priohyodus arambourgi* (Hybodontiformes: Hybodontidae) from Late Jurassic-?earliest Cretaceous deposits in Uruguay: *Cretaceous Research*, v. 35, p. 118–123, doi:10.1016/j.cretres.2011.12.001.
- SOTO, M., TORINO, P., AND PEREA, D., 2020, A large sized megalosaurid (Theropoda, Tetanuriae) from the Late Jurassic of Uruguay and Tanzania: *Journal of South American Earth Sciences*, v. 98, p. 102458, doi:10.1016/j.jsames.2019.102458.
- SPALLETTI, L.A., AND PINOL, F.C., 2005, From alluvial fan to playa: an Upper Jurassic ephemeral fluvial system, Neuquén Basin, Argentina: *Gondwana Research*, v. 8, p. 363–383, doi:10.1016/S1342-937X(05)71141-2.
- TANDON, S.K., GIBLING, M.R., SINHA, R., SINGH, V., GHAZANFARI, P., DASGUPTA, A., JAIN, M., AND JAIN, V., 2006, Alluvial Valleys of the Ganga Plains, India: Timing and Causes of incision, in Dalrymple, R.W., Leckie, D.A., and Tillman, R.W., eds., *Incised Valleys in Time and Space: SEPM, Special Publication 87*, p. 15–35.
- TODD, S.P., 1996, Process deduction from fluvial sedimentary structures, in Carling, P.A., and Dawson, M.R., eds., *Advances in Fluvial Dynamics and Stratigraphy*: John Wiley and Sons, p. 299–350.
- TURNER, P., 1980, *Continental Red Beds*: Elsevier, 562 p.
- VEIGA, G.D., AND SPALLETTI, L.A., 2007, The Upper Jurassic (Kimmeridgian) fluvial-aeolian systems of the southern Neuquén Basin, Argentina: *Gondwana Research*, v. 11, p. 286–302, doi:10.1016/j.gr.2006.05.002.
- VENTRA, D., AND CLARKE, L.E., 2018, Geology and geomorphology of alluvial and fluvial fans: current progress and research perspectives, in Ventra, D., and Clarke, L.E., eds., *Geology and Geomorphology of Alluvial and Fluvial Fans: Geological Society of London, Special Publication 440*, p. 1–21, doi:10.1144/SP440.16.
- WALKER, R.G., AND JAMES, N.P., 1992, Facies Models: Response to Sea Level Change: Geological Association of Canada, 454 p.

- WANG, J., AND PLINK-BJÖRKUND, P., 2019, Stratigraphic complexity in fluvial fans: Lower Eocene Green River Formation, Uinta Basin, USA: *Basin Research*, v. 31, p. 892–919, doi:10.1111/bre.12350.
- WEISSMANN, G.S., MOUNT, J.F., AND FOGG, G.E., 2002, Glacially driven cycles in accumulation space and sequence stratigraphy of a stream-dominated alluvial fan, San Joaquin Valley, California, U.S.A.: *Journal of Sedimentary Research*, v. 72, p. 240–251, doi:10.1306/062201720240.
- WEISSMANN, G.S., BENNETT, G.L., AND LANSDALE, A.L., 2005, Factors controlling sequence development on Quaternary fluvial fans, San Joaquin Basin, California, in Harvey, A.M., Mather, A.E., and Stokes, M., Alluvial Fans: Geomorphology, Sedimentology, Dynamics, USA: Geological Society of London, Special Publication 251, p. 169–186, doi:10.1144/GSL.SP2005.251.01.12.
- WEISSMANN, G.S., HARTLEY, A.J., NICHOLS, G.J., SCUDERI, L.A., OLSON, M., BUEHLER, H., AND BANTEAH, R., 2010, Fluvial form in modern continental sedimentary basins: distributive fluvial systems: *Geology*, v. 38, p. 39–42, doi:10.1130/G30242.1.
- WEISSMANN, G.S., HARTLEY, A.J., SCUDERI, L.A., NICHOLS, G.J., DAVIDSON, S.K., OWEN, A., ATCHLEY, S.C., BHATTACHARYA, P., CHAKRABORTY, T., GHOSI, P., NORDT, L.C., MICHEL, L., AND TABOR, N.J., 2013, Prograding distributive fluvial systems: geomorphic models and ancient examples, in Driese, S.G., and Nordt, L.C., eds., New Frontiers in Paleopedology and Terrestrial Paleoclimatology: SEPM, Special Publication 104, p. 131–147.
- WEISSMANN, G.S., HARTLEY, A.J., SCUDERI, L.A., NICHOLS, G.J., OWEN, A., WRIGHT, S., FELICIA, A.L., HOLLAND, F., AND ANAYA, F.M.L., 2015, Fluvial geomorphic elements in modern sedimentary basins and their potential preservation in the rock record: a review: *Geomorphology*, v. 250, p. 187–219, doi:10.1016/j.geomorph.2015.09.005.
- WIZEVICH, M.C., 1993, Depositional controls in a bedload-dominated fluvial system: internal architecture of the Lee Formation, Kentucky: *Sedimentary Geology*, v. 85, p. 537–556, doi:10.1016/0037-0738(93)90101-A.
- YANBIN, S., GALLEGOS, O.F., AND MARTÍNEZ, S., 2004, The conchostracean subgenus *Orthetheria (Migransia)* from the Tacuarembó Formation (Late Jurassic–?Early Cretaceous, Uruguay) with notes on its geological age: *Journal of South American Earth Sciences*, v. 16, p. 615–622, doi:10.1016/j.jsames.2003.02.001.
- ZALÁN, P.V., WOLFF, S., CONCEIÇÃO, J.C.J., ASTOLFI, M.A.M., VIEIRA, I.S., APPI, V.T., AND ZANOTTO, O.A., 1987, Tectônica e sedimentação da Bacia do Paraná, in Atas Do III Simpósio Sul-Brasileiro de Geologia: Curitiba, Sociedade Brasileira de Geologia, p. 441–447.

Received 22 April 2021; accepted 1 February 2022.